AD-A173 577 INVESTIGATION OF DEVICE AND ELECTRONIC INTERACTIONS ASSOCIATED WITH GAAS (U) MASSACHUSETTS INST OF TECH CAMBRIDGE DEPT OF MATERIALS SCIENC H C GATOS ET AL 1/1

UNCLASSIFIED 15 AUG 85 AFOSR-TR-85-1033 F49620-83-C-0139 F/G 20/12 NL

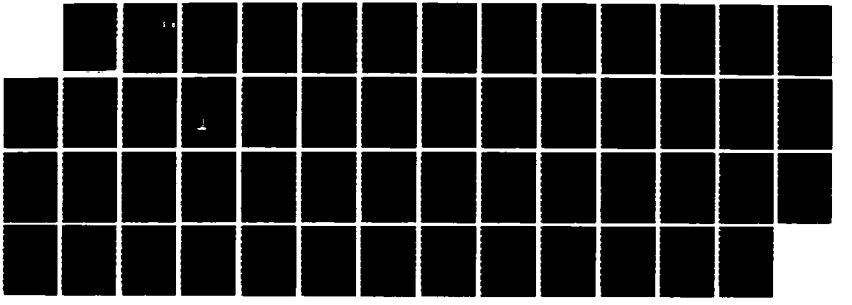

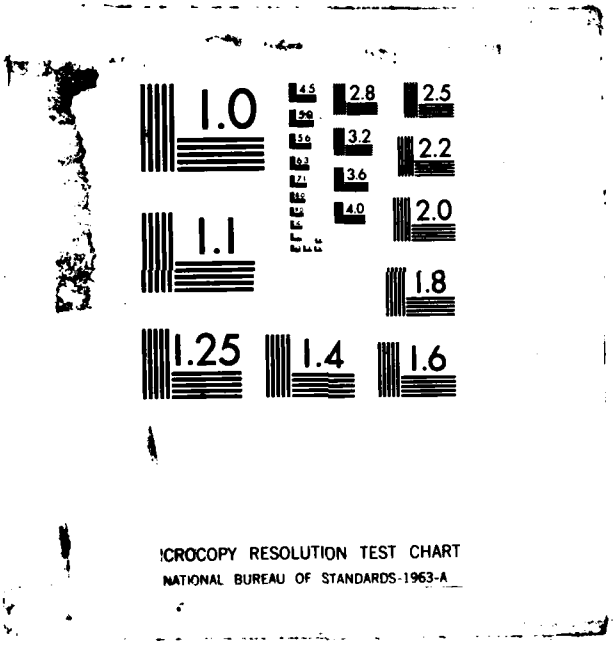
1.0
1.1
1.25
2.8
3.2
3.6
4.0
2.5
2.2
2.0
1.8
1.4
1.6
ICROCOPY RESOLUTION TEST CHART
NATIONAL BUREAU OF STANDARDS-1963-A

ANNUAL TECHNICAL REPORT

to

AIR FORCE OFFICE OF SCIENTIFIC RESEARCH
BOLLING AIR FORCE BASE, D. C. 20332

on

INVESTIGATION OF DEFECT AND ELECTRONIC INTERACTIONS ASSOCIATED WITH GaAs DEVICE PROCESSING

(F49620-83-C-0139)

For Period

August 15, 1984 to August 14, 1985

Submitted by

Professor Harry C. Gatos
and
Dr. Jacek Lagowski
Department of Materials Science and Engineering
Massachusetts Institute of Technology
Cambridge, Massachusetts 02139

Unc

SECURITY CLASSIFICATION OF THIS PAGE

AD-A173 577

REPORT DOCUMENTATION PAGE

1a REPORT SECURITY CLASSIFICATION	1b RESTRICTIVE MARKINGS
2a SECURITY CLASSIFICATION AUTHORITY	3. DISTRIBUTION/AVAILABILITY OF REPORT
2b DECLASSIFICATION/DOWNGRADING SCHEDULE	
4 PERFORMING ORGANIZATION REPORT NUMBER(S)	5. MONITORING ORGANIZATION REPORT NUMBER(S) AFOSR-TR-85-1033
6a NAME OF PERFORMING ORGANIZATION Massachusetts Institute of Technology / 6b. OFFICE SYMBOL (If applicable)	7a. NAME OF MONITORING ORGANIZATION same as # 8
6c. ADDRESS (City, State and ZIP Code) Cambridge, Massachusetts 02139	7b. ADDRESS (City, State and ZIP Code) same as #8
8a NAME OF FUNDING/SPONSORING ORGANIZATION AFOSR / 8b. OFFICE SYMBOL (If applicable) NE	9. PROCUREMENT INSTRUMENT IDENTIFICATION NUMBER F49620-83-C-0139
8c ADDRESS (City, State and ZIP Code) Building 410 Bolling AFB, D.C. 20332	10 SOURCE OF FUNDING NOS: PROGRAM ELEMENT NO. 61102F; PROJECT NO. 2306; TASK NO. B1; WORK UNIT NO.
11 TITLE (Include Security Classification) Investigation of Device & Electron. Interactions in GaAs	
12. PERSONAL AUTHOR(S) Professor Harry C. Gatos and Dr. Jacek Lagowski	
13a. TYPE OF REPORT Annual / 13b. TIME COVERED FROM 8/15/84 TO 8/14/85	14 DATE OF REPORT (Yr., Mo., Day) August 15, 1985 / 15 PAGE COUNT 7
16. SUPPLEMENTARY NOTATION	

17. COSATI CODES			18 SUBJECT TERMS (Continue on reverse if necessary and identify by block number)
FIELD	GROUP	SUB GR	
			Sub, Ga ... As, ...

19. ABSTRACT (Continue on reverse if necessary and identify by block number)

We have pursued our investigation of defect and electronic interactions in GaAs along three lines especially important for device processing: (a) origin and control of native midgap levels; (b) feasibility for achieving vanadium-doped semi-insulating GaAs; and (c) origin and control of dislocations.

Employing DLTS measurements on p-type bulk GaAs crystals grown under different arsenic pressure, we have identified a dominant hole trap which exhibits two charge states at 0.54 eV and 0.77 eV above the valence band. These levels are most likely due to the single and double donor levels of the arsenic antisite As_{Ga} defect. The same samples are currently analyzed by photoluminescence at the Avionics Laboratory of Wright-Patterson Airforce Base in order to correlate deep level luminescence spectra with transient capacitance spectra. Our study of vanadium-doped GaAs has led to identification of the vanadium acceptor state $V^{-/2-}_{Ga}(3d^3)$ at 0.15 eV below the conduction band. No midgap levels other than EL2 could be detected, showing that vanadium plays no direct role in the compensation process in SI GaAs.

20 DISTRIBUTION/AVAILABILITY OF ABSTRACT UNCLASSIFIED/UNLIMITED ☒ SAME AS RPT. ☐ DTIC USERS ☐	21. ABSTRACT SECURITY CLASSIFICATION Unc
22a. NAME OF RESPONSIBLE INDIVIDUAL Capt. Kevin Malloy	22b. TELEPHONE NUMBER (Include Area Code) (202) 767-4931 / 22c. OFFICE SYMBOL NE

DD FORM 1473, 83 APR EDITION OF 1 JAN 73 IS OBSOLETE.

Unc

SECURITY CLASSIFICATION OF THIS PAGE

19. continued

in SI GaAs.

Using GaAs crystals doped with In and grown under different As pressure, we have obtained the first experimental evidence for a decrease in point defect concentration induced by isoelectronic doping. These results provided a basis for the heterogeneous dislocation generation model in which vacancy clusters play the role of generation sites for a dislocation network including the dislocations induced by thermal stress.

The results of our activity are outlined and they are discussed in detail in five publications enclosed with this report.

I. SUMMARY

We have pursued our investigation of defect and electronic interactions in GaAs along three lines especially important for device processing: (a) origin and control of native midgap levels; (b) feasibility for achieving vanadium-doped semi-insulating GaAs; and (c) origin and control of dislocations.

Employing DLTS measurements on p-type bulk GaAs crystals grown under different arsenic pressure, we have identified a dominant hole trap which exhibits two charge states at 0.54 eV and 0.77 eV above the valence band. These levels are most likely due to the single and double donor levels of the arsenic antisite As_{Ga} defect. The same samples are currently analyzed by photoluminescence at the Avionics Laboratory of Wright-Patterson Airforce Base in order to correlate deep level luminescence spectra with transient capacitance spectra. Our study of vanadium-doped GaAs has led to identification of the vanadium acceptor state $V^{2+}(3d^3)$ at 0.15 eV below the conduction band. No midgap levels other than EL2 could be detected, showing that vanadium plays no direct role in the compensation process in SI GaAs.

Using GaAs crystals doped with In and grown under different As pressure, we have obtained the first experimental evidence for a decrease in point defect concentration induced by isoelectronic doping. These results provided a basis for the heterogeneous dislocation generation model in which vacancy clusters play the role of generation sites for a dislocation network including the dislocations induced by thermal stress.

The results of our activity are outlined below and they are discussed in detail in five publications enclosed with this report.

II. NATIVE DEEP LEVELS

We have identified a dominant hole trap in p-type bulk GaAs employing deep level transient and photocapacitance spectroscopies. The trap concentration

ranges from 2 x $10^{16}cm^{-3}$ to 7 x $10^{16}cm^{-3}$, and it increases with increasing arsenic pressure in the growth ampule. The trap has two charge states with energies 0.54 $\pm$ 0.02 and 0.77 $\pm$ 0.02 eV above the top of the valence band (at 77 K) which are clearly visible in the steady state photocapacitance spectrum of Fig. 1. From the upper level the trap can be photoexcited to a persistent metastable state just as the dominant midgap level, EL2. Impurity analysis and the photoionization characteristics rule out association of the trap with impurities Fe, Cu, or Mn. Taking into consideration theoretical results, it appears most likely that the two charge states of the trap are the single and double donor levels of the arsenic antisite As_{Ga} defect. The identification of a native hole trap in GaAs associated with a double charge donor, provides the missing experimental link for establishing a working model of the As_{Ga} defect and understanding its role in the presence and in the characteristics of the dominant deep levels in GaAs. The study will be pursued in conjunction with deep level photoluminescenc measurements in order to further explain the properties of native midgap levels.

III. ROLE OF VANADIUM IN ATTAINING SI GaAs

In the present study we identified a vanadium-related electron trap in melt-grown GaAs by both DLTS and capacitance transient analysis. The samples studied were cut from LEC GaAs crystals grown in this laboratory using PBN crucibles from melts doped with high purity elemental vanadium to a level of 3 x $10^{19}cm^{-3}$. In addition, selenium doping of the melt up to about 9 x $10^{16}cm^{-3}$ was used to insure n-type conducting material.

Typical DLTS spectra in the range 100-420 K for crystals with and without vanadium are shown in Fig. 2. The dominant midgap level EL2 is clearly visible in both spectra at $\sim$390 K having a concentration of about 2 x $10^{16}cm^{-3}$. No additional midgap levels could be detected. In the V-doped material, however,

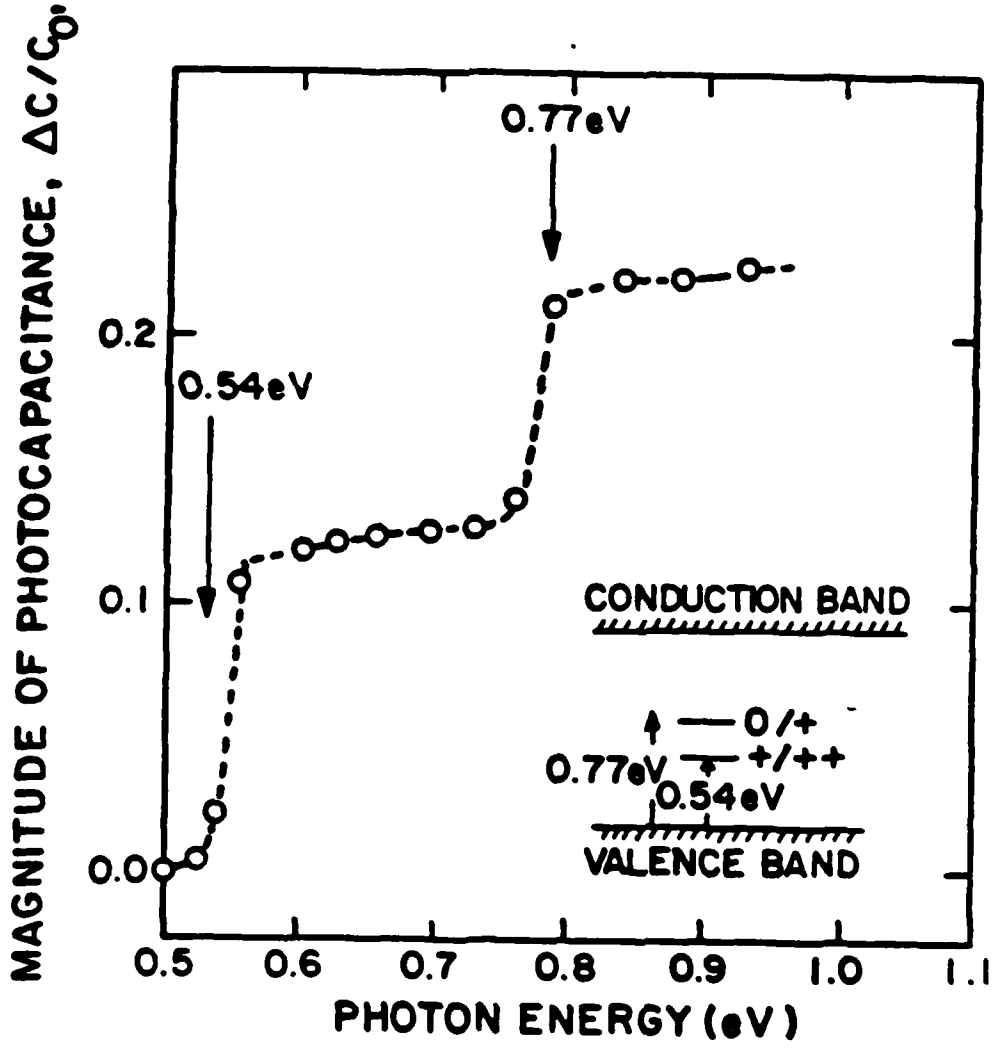

Fig. 1. Low temperature (77 K) spectrum of steady state photocapacitance corresponding to photoionization of two charge states of the native hole trap in GaAs.

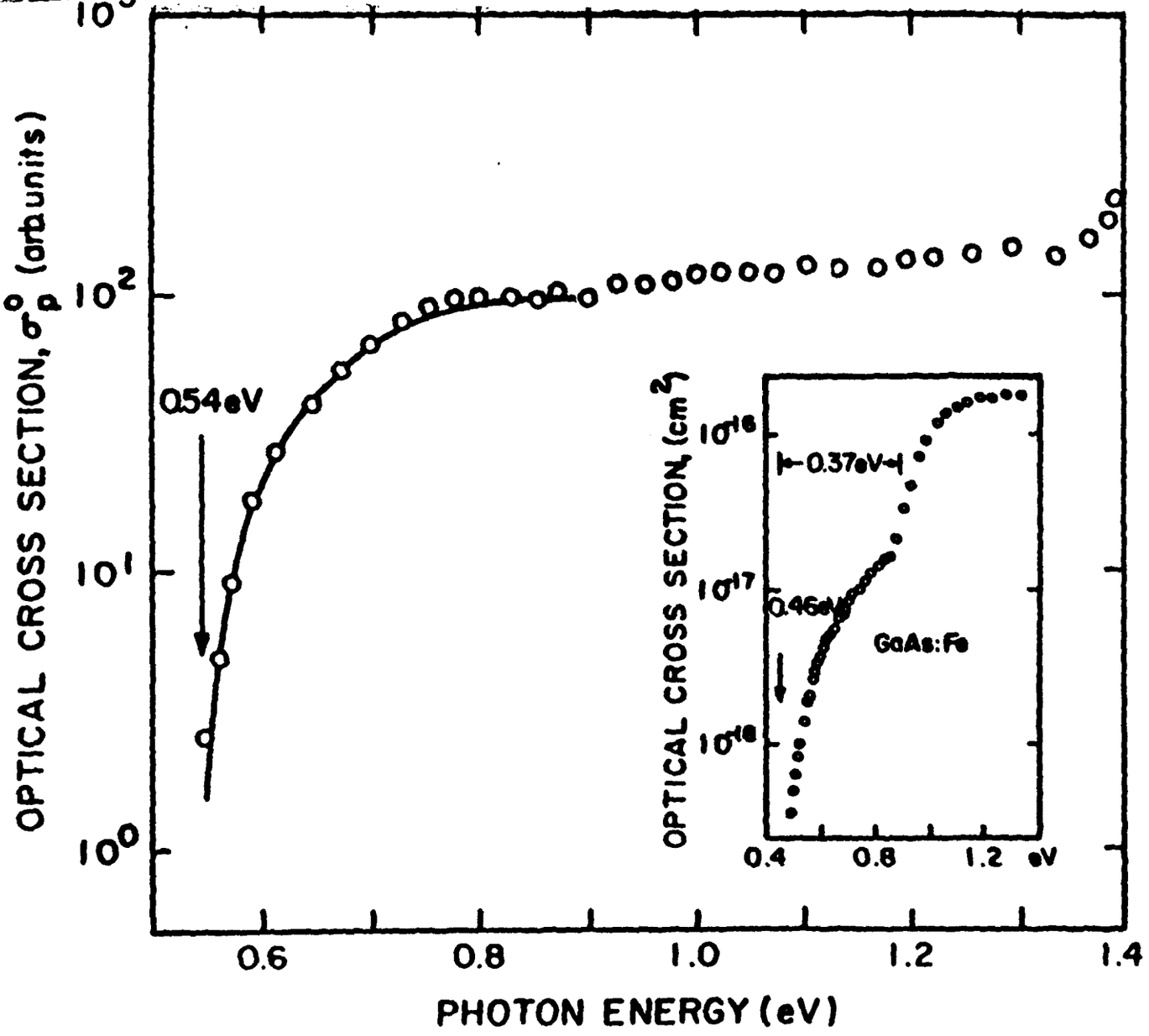
OPTICAL CROSS SECTION, σ_p^o (arbunits)
10^2
10^1
10^0
0.54eV
0.6
0.8
1.0
1.2
1.4
PHOTON ENERGY (eV)
OPTICAL CROSS SECTION, (cm^2)
10^{18}
10^{17}
10^{16}
0.37eV
0.46eV
GaAs:Fe
0.4
0.8
1.2
eV

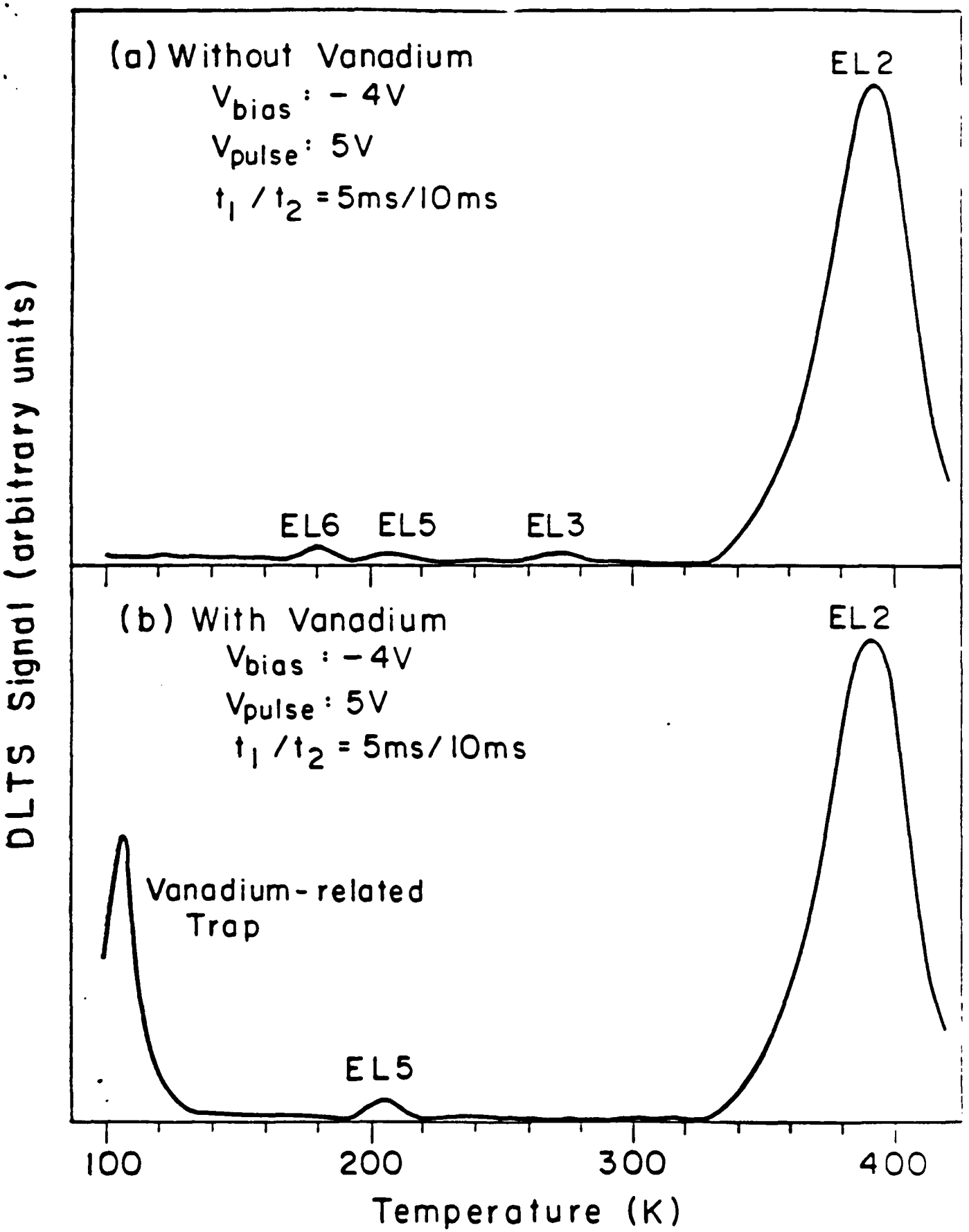

Fig. 2. DLTS spectra of n-type LEC-grown GaAs without (a) and with (b) vanadium doping. Bias -4V; filling pulse amplitude - 5V; t_1/t_2 = 5ms/10ms.

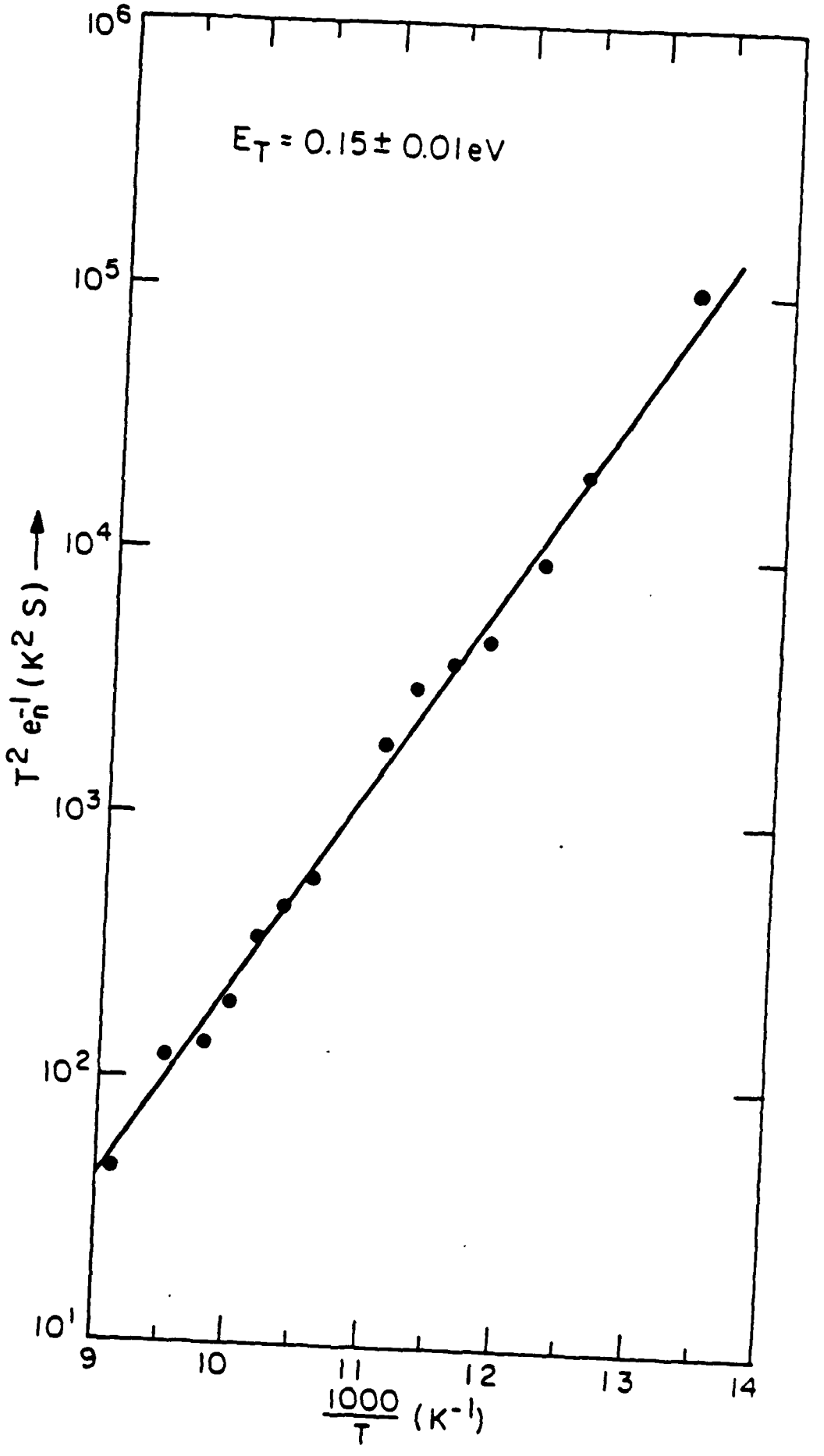
$E_T = 0.15 \pm 0.01$ eV
10^6
10^5
10^4
10^3
10^2
10^1
$T^2 e_n^{-1}$ (K^2 S) ⟶
9
10
11
12
13
14
$\frac{1000}{T}$ (K^{-1})

a new well pronounced peak appeared at ~100 K, indicating the presence of a new vanadium-related electron trap. Detailed capacitance transient analysis yielded a trap energy of 0.15 ± 0.01 eV below the conduction band and an electron capture cross section of about $2 \times 10^{-14} cm^2$. Optical absorption and mobility data show that this level corresponds to the ionized acceptor state $V^{2+}(3d^3)$ of substitutional vanadium. The concentration of this level enabled us to estimate the effective distribution coefficient of elemental vanadium in melt-grown GaAs to be about 2×10^{-4}.

The proximity of the vanadium acceptor level to the conduction band and the absence of any vanadium-related midgap levels strongly imply that the isolated vanadium atoms cannot play any direct role in obtaining SI material. Further studies to ascertain the potential involvement of vanadium, perhaps in the form of complexes with other impurities, in producing SI GaAs are in progress.

IV. UNIFIED MODEL OF HETEROGENEOUS DISLOCATION GENERATION IN GaAs

Employing GaAs crystals grown by the Horizontal Bridgman method under negligible thermal stress and under precisely controlled (varied) stoichiometry, we found that doping with In at concentrations exceeding $10^{18} cm^{-3}$ significantly decreases (by two orders of magnitude) the dislocation density in crystals grown under off-stoichiometry Ga-rich and As-rich conditions. In p-type crystals In-doping was also found to reduce the magnitude of Fermi level enhancement of vacancy condensation into dislocation loops. These results provide the first experimental evidence for a decrease in point defect concentration induced by isoelectronic doping and its profound consequences for dislocation generation. (Under stoichiometric conditions the dislocation density is very low even in the absence of any intentional doping.) They led us to the formulation of a comprehensive model of heterogeneous dislocation generation in GaAs in which vacancy clusters play the role of generation sites for dislocation network

including the dislocations induced by thermal stress. Utilizing this model we were able to explain extensive experimental data for GaAs crystals grown under intermediate and low thermal gradients:

(1) existence of a distinct minimum of dislocation density vs. the stoichiometry of the growth melt;

(2) suppression of dislocation density by intermediate level n-type doping ($\sim 10^{17} cm^{-3}$)

(3) enhancement of dislocation density by intermediate level p-type doping ($\sim 10^{17} cm^{-3}$);

(4) dependence of the critical stress for dislocation generation on the melt stoichiometry;

(5) highly diversified experimental reports on correlation, anticorrelation, or lack of correlation between the dislocation density and the EL2 concentration.

Our model is currently being tested using a TEM study of dislocation loops vs. melt stoichiometry in melt-grown GaAs.

V. PUBLICATIONS ENCLOSED WITH THIS REPORT

1. J. Lagowski and H.C. Gatos, "Nonstoichometric Defects in GaAs and the EL2 Bandwagon," 13th Int. Conf. on Defects in Semiconductors, Coronado, CA, 1984, edited by L.C. Kimerling and J.M. Parsey, Jr., The Metallurgical Soc. of AIME, 1985, p. 73.

2. H.C. Gatos and J. Lagowski, "EL2 and Related Defects in GaAs--Challenges and Pitfalls," Proc. of MRS Symp. on "Microscopic Identification of Electronic Defects in Semiconductors," April 1985, San Francisco, CA.

3. C.-J. Li, Q. Sun, J. Lagowski and H.C. Gatos, "EBIC Spectroscopy--A New Approach to Microscale Characterization of Deep Levels in SI-GaAs,"

Proc. of MRS Symp. on "Microscopic Identification of Electronic Defects in Semiconductors," April 1985, San Francisco, CA.

4. C.D. Brandt, A.M. Hennel, L.M. Pawlowicz, F.P. Dabkowski, J. Lagowski and H.C. Gatos, "Identification of a Vanadium-Related Level in LEC-Grown GaAs," Appl. Phys. Lett., 1985, in press.

5. J. Lagowski, D.G. Lin, T.-P. Chen, M. Skowronski and H.C. Gatos, "On a Native Trap in Bulk GaAs and Its Association with the Double-Charge State of the Arsenic Antisite Defect," submitted to Applied Physics Letters.

Thirteenth International Conference on Defects in Semiconductors, Aug. 12-17,1984, Coronado, CA, edited by L.C. Kimerling and J.M. Parsey, Jr., The Metallurgical Society of AIME, Warrendale, PA, 1985.

NONSTOICHIOMETRIC DEFECTS IN GaAs AND THE EL2 BANDWAGON

Jacek Lagowski and Harry C. Gatos

Massachusetts Institute of Technology
Cambridge, Massachusetts 02139

Abstract

Native defects, whose formation is enhanced by deviations from melt stoichiometry, can be either detrimental or beneficial to GaAs IC technology. Detrimental effects originate in the high dislocation densities present in crystals grown under nonstoichiometric conditions. Beneficial effects are encountered in the compensation mechanism in undoped semi-insulating (SI) GaAs grown from As-rich melts. Among the defects that might be involved in such a mechanism the deep native donor EL2 has started a "bandwagon". Optical and paramagnetic properties of EL2 have been found compatible with an isolated antisite defect As_{Ga}. However, such an assignment turned out to be inconsistent with current high resolution studies. This outcome is not surprising if one considers that properties attributed to EL2 originate from additional deep levels (EL2 family!) with very similar energy positions.

In this paper we seek the clarification of native defects by pursuing relationships between EL2, dislocations, and melt stoichiometry in a framework of defect equilibria which define the defect concentrations in the solidifying crystal. Post-solidification processes (i.e., migration of defects and their condensation into dislocations and dislocation climb) are distinguished from solidification proper because of their unique dependence on the Fermi energy, i.e., on the charge state of the defects.

I. Introduction

The importance of melt stoichiometry in the growth of GaAs crystals has been recognized since the early 60's, primarily in conjunction with preventive measures undertaken to minimize the loss of arsenic. The B_2O_3 liquid encapsulation technique (Czochralski method) and the control of the As pressure by the arsenic source temperature (Bridgman method) were developed and remain the practical solutions to the arsenic volatility. The early studies of stoichiometry effects on the properties of GaAs were sporadic and limited in scope (1-3). The situation changed dramatically in 1981-82 when the research groups of Rockwell International (4,5) and Westinghouse R&D Laboratories (6) demonstrated the materials engineering aspects of stoichiometry and had an immediate impact on GaAs IC technology. They have found that high purity GaAs crystals with very high resistivity and withstanding device processing at elevated temperatures can be reproducibly grown provided that the melt is

slightly enriched with arsenic.

In parallel, also in 1981-82, the MIT group demonstrated the crucial role of melt stoichiometry in minimizing the dislocation density (7). Furthermore, in the light of the effect of melt stoichiometry and donor impurities on the EL2 concentration they proposed the first antisite defect model of creation of the midgap level EL2 (8). Since then the interest in nonstoichiometric defects, and especially in EL2 and dislocations has been rapidly growing and has been fueled by device yield aspects on the one hand, and by the unique fundamental properties which had a rejuvenating effect on the stagnant semiconductor physics on the other.

Several dozen papers are published on EL2 and dislocations every year. Still, a critical review of the present state of knowledge is a complex task. The questions seem to outnumber the answers, and the research of today rapidly questions the "unambiguous" findings of yesterday. During the Lund Conference in Hungary in 1983, convincing arguments were presented for the EL2 identification as an isolated antisite defect As_{Ga}, which were based on new data on optical intracenter transitions and the splitting of the no-phonon line in uniaxial stresses (9). An EPR study on plastically deformed GaAs had also favored the same conclusions (10). However, high resolution measurements of the no-phonon line (11) and of the EPR line (12, 47) obtained only recently, show that both lines involve more than one defect!

It has been a prevailing trend to attribute the very high dislocation densities in GaAs to its poor mechanical strength and to excessive thermal stresses (13,14). Any significant effects of stoichiometry on the dislocation density (1,7,15) were clearly beyond the scope of such treatments. Only recently a striking relationship has been discovered between the dislocation density and the Fermi energy in melt-grown GaAs (6). This finding pointed directly to the importance of post-solidification interactions among charged point defects and helped to define the regimes of thermal stress, nonstoichiometry, isoelectronic doping and standard impurity hardening, all of which are of fundamental importance for controlling dislocations in GaAs.

The present paper is not a review of defects in GaAs. Instead, we attempt to formulate a common framework for a discussion of nonstoichiometric defects, especially EL2 and dislocations. Accordingly, we will outline the most important settled and unsettled issues. Our choice will be guided not only by fundamental interests, but also by urgent needs in advancing IC technology.

II. Stoichiometry-Controlled Compensation

It is now generally recognized that control of the melt stoichiometry is the key to the reproducible growth of "undoped" high quality semi-insulating GaAs. Results of the Rockwell and Westinghouse research groups (after refs. 5 and 6, respectively) presented in Fig. 1 show that high resistivity ($\rho > 10^7$ Ωcm) GaAs can be grown only in a narrow arsenic atom fraction range $0.47 < [As] < 0.52$. Most of this range yields low Hall effect mobility values (see Fig. 2) which correspond to a mixed conductivity or to p-type conductivity. High quality crystals with high mobilities, >5000 cm^2/Vs, are obtainable from melts slightly enriched with arsenic $[As] > 0.505$. Such crystals are certainly favored for IC processing since their wafers preserve their semi-insulating character upon thermal annealing used to activate electrical conductivity in regions subjected to ion implantation (6). The significantly enhanced thermal stability of "undoped" GaAs as compared to heavily Cr-doped GaAs constitutes a major advantage which has made an immediate impact on IC technology.

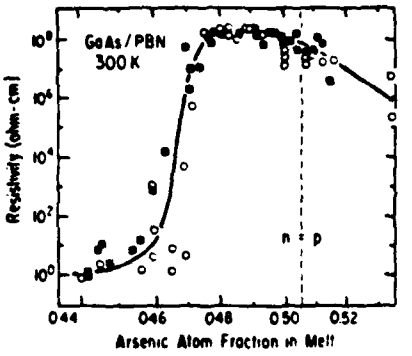

Fig. 1. Resistivity of undoped GaAs grown by the LEC method vs. the arsenic atom fraction in melt.
● - results of Westinghouse group;
o - results of Rockwell group.

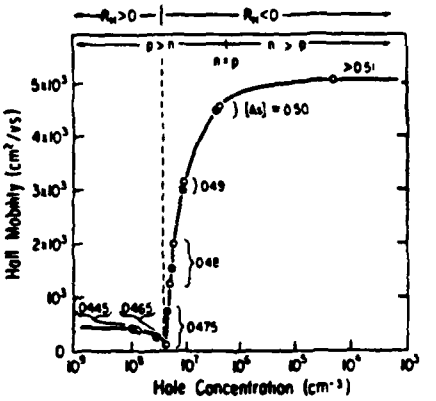

Fig. 2. Hall mobility data for LEC-grown GaAs which demonstrate p to n transition induced by enrichment of the melt with arsenic.
● - results of Westinghouse group;
o - results of Rockwell group.

The very high resistivity of "undoped" melt-grown GaAs is attributable to the balance between the net concentration of shallow acceptors and that of deep donors (17,18). This balance is upset when the arsenic fraction in the growth melt falls below a certain critical value. It is thus evident that point defects controlled by the arsenic activity at and near the melting point play an important role in achieving SI-GaAs (5). It is of interest to note that among the simple native atomic disorders only the antistructure can account for p-type or n-type conductivity change upon transition from Ga-rich to As-rich melt conditions (19). As shown in Table I, Schottky disorder would

Table I. Expected Role of Melt Stoichiometry in Electrical Conductivity for the Basic Atomic Disorders

Atomic Disorder	Ga-rich Melt		As-rich Melt	
	Dominant Defect	Conductivity Type	Dominant Defect	Conductivity Type
Schottky	V_{As}	n	V_{Ga}	p
Frenkel[A]	Ga_i	p	V_{Ga}	p
Frenkel[B]	V_{As}	n	As_i	n
Anti-structure	Ga_{As}	p	As_{Ga}	n

A,B - Disorder on gallium and arsenic sublattices, respectively.

lead to an opposite behavior, while Frenkel disorder on an arsenic sublattice would yield n-type conductivity on the Ga-rich side. The gallium antisite, Ga_{As} defect, responsible for p-type conductivity in Ga-rich growth, is indeed believed to be the native acceptor which, in addition to residual carbon impurities, plays a key role in the compensation mechanism of SI-GaAs (20).

The midgap donor involved in the compensation of shallow acceptors was commonly identified with EL2 (17). This identification was based on the

presumption that a particular optical bleaching characteristic of SI-GaAs is the "fingerprint" of EL2 (21). According to the present state of knowledge, such identification is by no means a unique one. Midgap levels other than EL2 (e.g., the oxygen-related ELO level) have been observed in GaAs with energies and optical quenching characteristics very similar to those of EL2 (22-24).

A detailed assessment of the role of individual midgap levels in the compensation mechanism is one of the most important unsettled issues. This issue (discussed also in the following sections) bears directly on the origin of electrical, optical and structural inhomogeneities in SI-GaAs and upon the relationships (real and apparent, see next section) between spacial distributions of EL2 and the dislocation density in GaAs crystals. Macro- and microscopic inhomogeneities originating from melt stoichiometry variations during solidification and/or from defects induced by excessive thermal stresses during cooling of the crystals (25) constitute currently the most difficult materials problems in GaAs IC technology (26). High temperature annealing of the entire GaAs bulk (about 6 hours at 750-800°C) seems to provide a means for homogenization of SI-GaAs (27,28). However, the mechanisms involved in this empirical procedure have not been fully assessed as yet.

III. Defect Equilibria-Dislocations and EL2

Type and concentrations of native defects and their relationships with crystal growth are determined by the following major factors:

(a) elevated temperature necessary for the crystal growth promotes displacement of atoms creating a native atomic disorder;

(b) GaAs exhibits a finite existence region in which the solid contains different concentrations of gallium and arsenic atoms (it is not stoichiometric);

(c) during cooling the crystal becomes supersaturated with defects which migrate, recombine, interact, form complexes, coalesce into dislocations, and participate in dislocation climb;

(d) excessive thermal stresses present in the growing crystal generate dislocations and point defects.

The above factors and the corresponding temperature ranges are shown schematically in Fig. 3 during Czochralski growth. Factors (a) and (b)

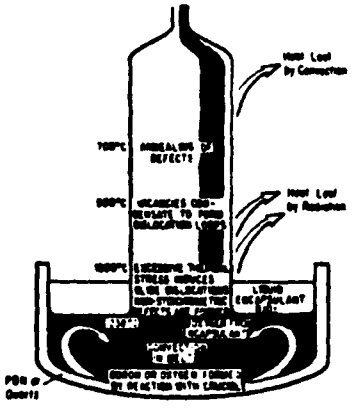

Fig. 3. Defect evolution during LEC growth of GaAs.

provide a starting point in the description of defect equilibria in melt-grown GaAs; the effects of melt stoichiometry and arsenic pressure are contained in factor (b). Theoretical data on GaAs solidus shown in Fig. 4 were calculated for simple atomic disorders, namely: Schottky disorder (29);

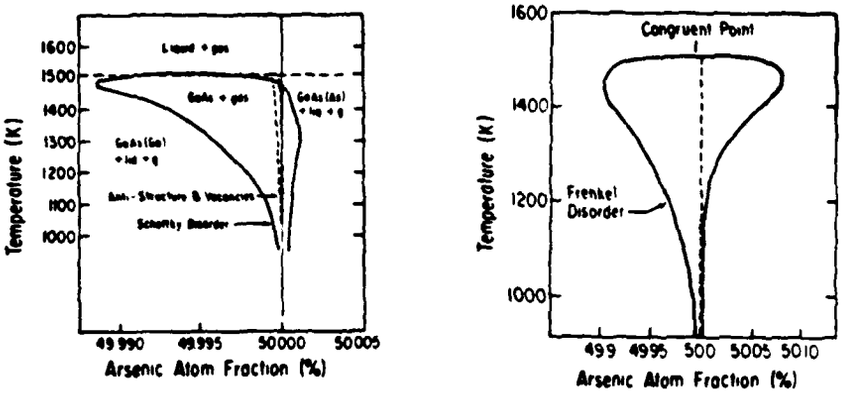

Fig. 4. Theoretical data on GaAs solidus (after ref. 29-31); (see text).

Frenkel disorder (30), and for a combination of antistructure and vacancies (31). The extent of the existence region (defined as the width of the solidus) is dramatically different for each calculation. In our opinion, two orders of magnitude differences in Fig. 4 reflect inaccuracies in theoretical calculations rather than differences in models of atomic disorder. Theoretical and experimental data on GaAs nonstoichiometry, δ, are presented in Fig. 5 as a function of arsenic fraction in the melt after ref. 30 and ref. 3, respectively.

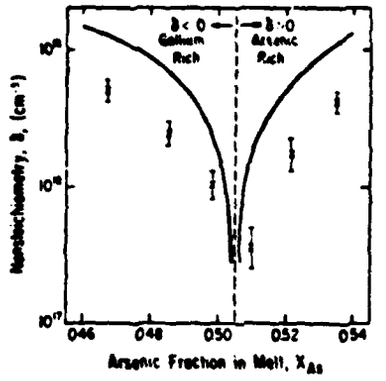

Fig. 5. Theoretical (line-ref. 30) and experimental (points-ref. 3) results on GaAs nonstoichiometry.

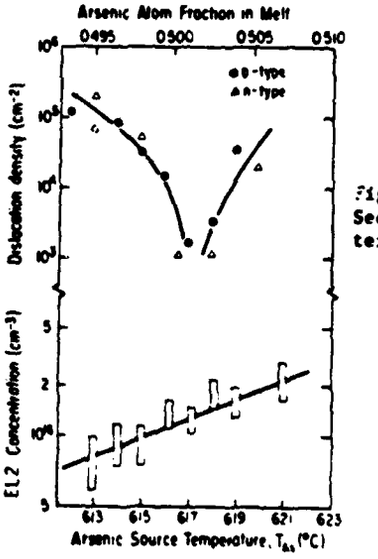

Fig. 6. See text.

Absolute values of δ contain a very large margin of uncertainty; they are, however, probably fairly accurate in assigning the optimum stoichiometry conditions to a slightly arsenic-rich melt composition.

Results of the MIT group (32,16) for horizontal Bridgman (HB) growth of GaAs with the melt stoichiometry varied by changing the temperature of the arsenic source, T_{As}, have shown that the dislocation density responds to the changes in melt composition in a way which is very similar to the behavior of the nonstoichiometry, δ. As shown in Fig. 6, a pronounced minimum of the dislocation density is obtained in crystals grown under optimum conditions defined by T_{As}=617±0.5°C and/or by the corresponding arsenic atom fraction in the melt slightly exceeding 0.50. It is also seen in Fig. 6 that the EL2 concentration increases monotonically with increasing arsenic fraction in the melt (8). This dependence is consistent with the assignment of EL2 to the arsenic antisite As_{Ga}.

Defect interactions during post-solidification cooling, factor (C), were not considered in defect equilibria models discussed above. These processes, however are of paramount importance regarding the final defect state in as-grown GaAs crystals (33). Post-solidification processes can be identified and distinguished from processes concurrent with solidification due to their dependence on the Fermi energy. At the melting point temperature (1238°C) the intrinsic carrier concentration, n_i, in GaAs is as high as $3\times10^{18}cm^{-3}$, and the Fermi energy cannot be changed by intentional doping at a moderate level of about 10^{17} cm^{-3}. However, at lower temperatures experienced by the crystal during cooling n_i decreases significantly and it becomes possible to vary the Fermi energy by moderate doping and thus change the charge state of the defects and their tendency to coalesce and migrate. The experimental dependence of the EL2 concentration and of the dislocation density on free carrier concentration (measured at 300 K) in HB GaAs crystals (grown under optimum T_{As}) is shown in Fig. 7, together with the corresponding

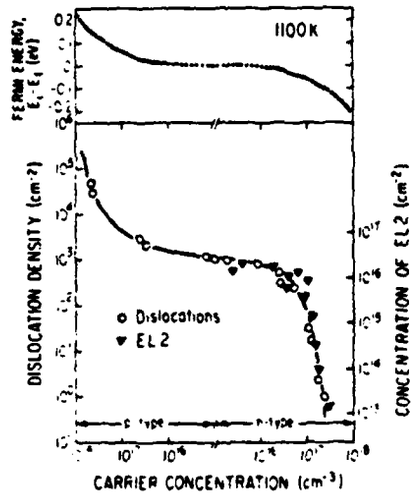

Fig. 7. See text.

Fermi energy change at an elevated temperature of 1100 K, which is believed to be a critical temperature for defect interactions (8,16). It is seen that for a shift of the Fermi energy from 0.1 eV above to 0.2 eV below its intrinsic value, the dislocation density increases by as much as five orders of magnitude. n-type doping at a level of about $10^{17}cm^{-3}$ (i.e., more than one order of magnitude below the doping levels utilized in standard impurity hardening phenomena (15) leads to a remarkable decrease of the EL2 concentration, very similar to the suppression of the dislocation density. It is conceivable that both effects originate from the migration of V_{Ga} to a neighboring arsenic site, As_{As}, which creates the arsenic antisite As_{Ga} and arsenic vacancy V_{As}:

$$V_{Ga}^{---} + As_{As} \rightleftarrows As_{Ga}^{+} + V_{As}^{+} + 4e^{-} \qquad (1)$$

This reaction proceeding from left to right is rapidly suppressed by the increase of free electron concentration ($\propto n^{-4}$). The annihilation of EL2

(explained in terms of reaction 1) provided the very first argument for the association of EL2 (directly or in the form of a complex) with the arsenic antisite defect. The corresponding reduction of the dislocation density was explained in terms of the rapid reduction of arsenic vacancies required for dislocation climb (34) and the concurrent increase of charged gallium vacancies which cannot condense (16). The monotonic increase of the EL2 concentration under As-rich melt growth (Fig. 6) is attributed to the increased concentration of $[V_{Ga}]$. The explanation of the dislocation minimum at optimum stoichiometric conditions is more complex, and it involves defect condensation into dislocation loops as well as subsequent dislocation climb.

Excessive thermal stresses in the solidified crystal represent an external factor which is beyond thermodynamic treatments of defect equilibria. Such stresses can by themselves generate dislocations (13) and antisite defects (10). However, the effects of thermal stresses can be enhanced by point defects which are required to maintain dislocation climb and/or form generation sites for dislocations (heterogeneous process) (35). On the other hand, optimum stoichiometric conditions and low defect concentrations increase the critical stress required to generate dislocations (homogeneous process) and effectively prevent dislocation climb.

IV. Current Issues Pertaining to the Identification of EL2

The questions as to whether or not and how EL2 is related to the antisite defect, As_{Ga}, have generated a great deal of interest. The argumentation based on EPR studies is presented in these proceedings in a separate paper (12). Accordingly, we will discuss the optical absorption studies (9) which were originally treated as a unique evidence for the identification of EL2 with a neutral state of an isolated antisite center. The optical absorption attributed to EL2 contains a band of intracenter transitions with a no-phonon line and transverse acoustic phonon replicas (Fig. 8). This no-phonon line has been found to split under uniaxial stress depending on the direction of the stress, σ, and the light propagation, $\bar{S}$, and polarization. Representative experimental data are shown in Fig. 9, together with predictions based on the static crystal field theory. This theory permits no other interpretation of the observed splitting than: $A_1 \rightarrow T_2$ transitions. The lack of measurable magnetic field effects on the no-phonon line was taken to imply that the transitions take place between ground and excited states which are spin singlets. Therefore, these states were identified as $^1A_1$ and $^1T_2$, respectively. This result was an excellent agreement with the theoretical prediction of the arsenic antisite levels, i.e., $^1A_1$ ground state resonant with the conduction band (36.37).

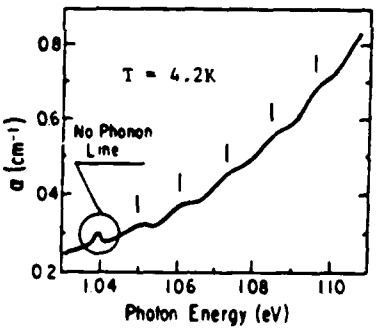

Fig. 8. Fine structure of the midgap level intracenter absorption. Ref. 9.

The above interpretation of the no-phonon line and its association with an isolated antisite defect is most likely correct. However, the conclusion that the EL2 is the isolated antisite is not necessarily valid. In Fig. 10 we present the intensity of the no-phonon line in crystals with different EL2 concentration (11). The lack of a unique relationship between the no-phonon

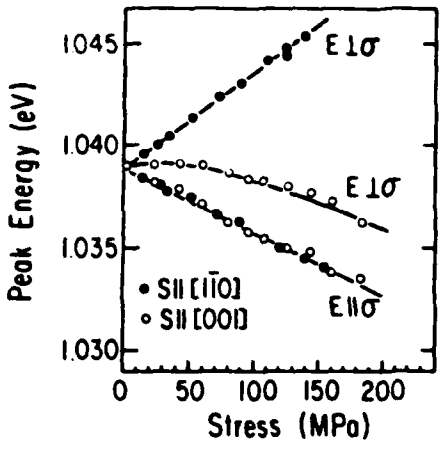

Fig. 9(a). No-phonon line behavior in uniaxial stress experimental results. After ref. 9.

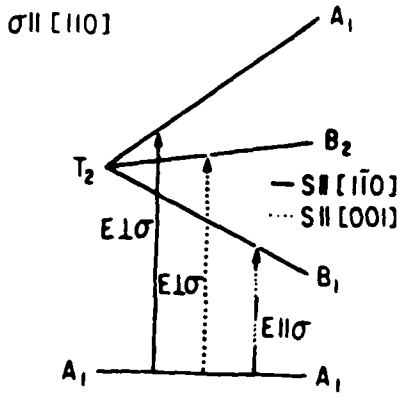

Fig. 9(b). Theoretical predictions based on the static crystal field theory. After ref. 9.

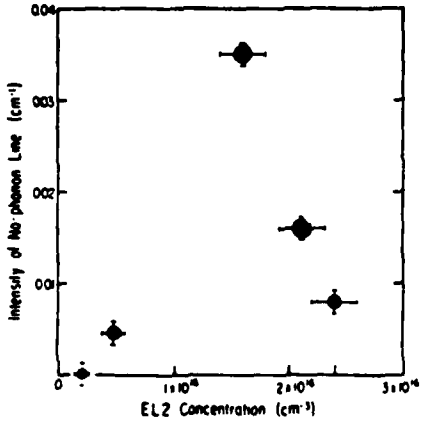

Fig. 10. Intensity of the no-phonon line vs. EL2 concentration. Highest intensity point corresponds to oxygen-doped GaAs which contains the two midgap levels EL2 and ELO. EL2 concentrations were determined by DLTS. Ref. 11.

line and EL2 is apparent. The high resolution measurements (11) performed on crystals with the strongest no-phonon line revealed a surprising line shape shown in Fig. 11. It is evident that the line shape can be better described by two symmetrical lines separated by about 1.5 meV rather than by a single asymmetrical no-phonon line, as previously assumed. The higher intensity line is probably due to the antisite defect As_{Ga}. The origin of the second line is not known. It also remains to be determined which of the component lines (if any) is uniquely related to EL2. It is of importance to note that in current high resolution EPR data the "line shape problem" was also encountered: the line, previously assigned to the paramagnetic state of a singly ionized isolated arsenic antisite, was shown to involve additional lines (12).

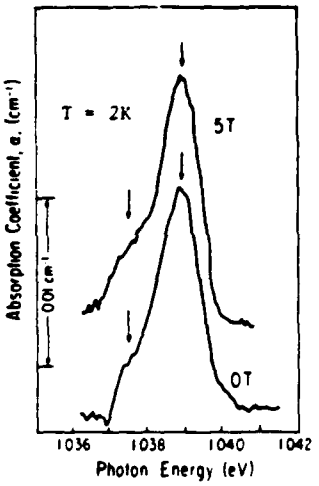

Fig. 11. Results of high resolution measurements of the no-phonon line in a magnetic field of 5T and without magnetic field (0T). Ref. 11.

The line-shape problems revealed by optical absorption and EPR studies must have a great deal in common with other recent surprising findings. Thus, it has been established with a high degree of confidence that EL2 is not the only midgap level in melt-grown GaAs (22-24,38). Other midgap levels are often present in LEC and in HB-GaAs at concentrations which depend on the exact growth condition. An "EL2 family"--i.e., a set of levels with activation energies very similar to those of EL2 but with different values of electron capture cross sections, was observed in LEC GaAs (22,23). All of these levels exhibited photocapacitance quenching effect, which was treated in the past as the "fingerprint" of EL2 (21,39). A study of HB-GaAs doped with oxygen (24) revealed the presence of an oxygen-related level, EL0, with emission characteristics shown in Fig. 12. A strong no-phonon line with a shape similar to that of the line shown in Fig. 11 was also present in oxygen-doped crystals. An electron capture cross section of EL0 about four times larger than that of EL2 (40) was found to be the only pronounced difference between the two levels. This difference is very important, however, because the relative EL0 contribution to the overall DLTS peak (or to capacitance transient) can be enhanced significantly by employing short duration filling pulses.

V. Dislocations--Current Issues

In Fig. 13 we have summarized the regimes of fundamental importance in the formation of dislocations in melt-grown GaAs. Two mechanisms of dislocation formation are distinguished: (1) stress-induced glide dislocations which are generated by excessive thermal stresses; and (2)nonstoichiometry-induced dislocations which are generated by the condensation of excess vacancies into dislocation loops. It should be emphasized that stress-induced dislocations are not independent of stoichiometry. They are in fact controlled to a large extent by defects participating in the climb process and/or by defects condensing into dislocation nucleation sites.

There are several means for obtaining dislocation-free GaAs employing precise stoichiometry control and/or doping with certain impurities. Isoelectronic doping with elements from group III or V has only recently

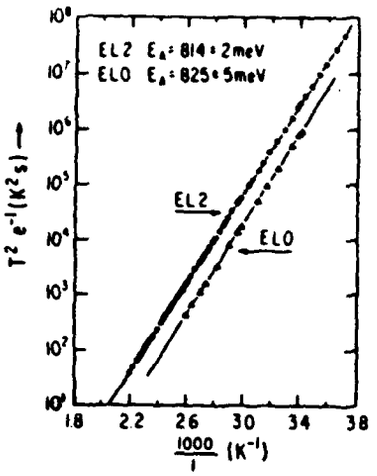

Fig. 12(a). Thermal emission of electrons from EL2 and ELO. Ref. 24.

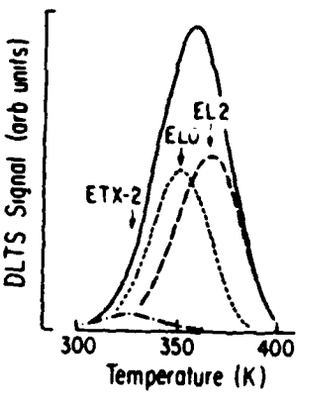

Fig. 12(b). Deconvoluted DLTS spectrum of oxygen-doped GaAs (rate window 25.6s^{-1}) Ref. 24.

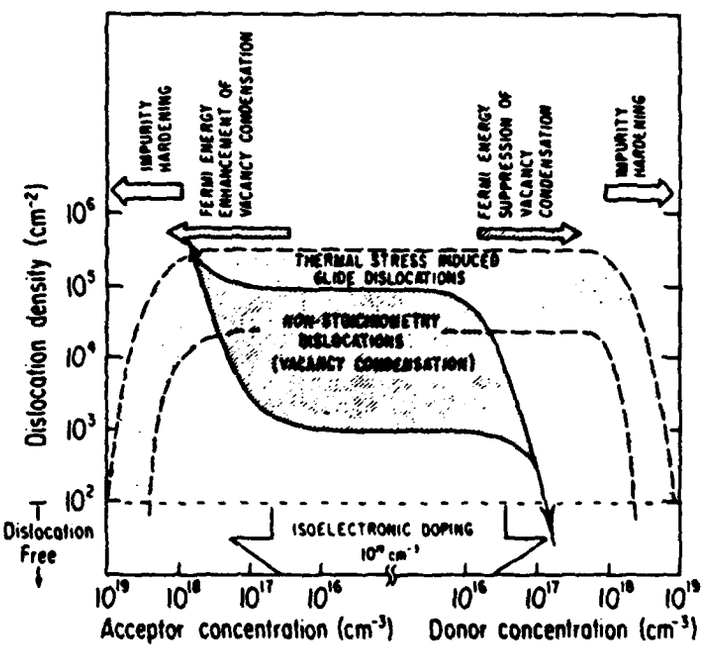

Fig. 13. Schematic diagram of the effects of impurities on the dislocation density in GaAs.

received a great deal of attention as an effective means for growing dislocation-free semi-insulating GaAs without altering appreciably the electronic properties (15,42,43). Indium if the most common dopant, although a reduction of the dislocation density has been observed for all isoelectronic

dopants which have been tried so far, i.e., B, N. Sb and Al. The similarity of the effects of all these elements suggests that the isoelectronic doping effect may be different than the standard impurity hardening whereby blocking the propagation of dislocations is the result of strong localized bonding (44) differences in tetrahedral radii between the impurity and the host atoms (45) and impurity-defect complexes (46). It seems to us more probable that the role of isoelectronic dopants is associated with the reduction of native defects below a certain critical value required to maintain an effective dislocation climb. Why the addition of group III or V elements would reduce the defect concentration in GaAs is not clear at all.

VI. Conclusions

Nonstoichiometric defects play a critical role in the electronic properties of GaAs and its electronic applications; very significant progress has been recently made in learning how to adjust melt stoichiometry in order to maximize its beneficial effects and minimize its detrimental ones; furthermore, control of dislocation densities has been enhanced, and homogenization of GaAs crystals by heat treatment of the entire bulk is now promising. These are very impressive empirical achievements; however, they clearly lack the underpinnings of a fundamental understanding. This situation does not stem from lack of interest in the fundamentals, but rather from the increased complexity of the issues involved.

Acknowledgement

The authors are grateful to the National Aeronautics and Space Administration and to the U.S. Air Force Office of Scientific Research for financial support.

References

1. J.C. Brice and G.D. King, Nature 209, 1346 (1966).

2. J.C. Brice, J. Crystal Growth 7, 9 (1970).

3. V.T. Bublik, V.V. Karataev, R.S. Kulagin, M.G. Mil'vidskii, V.B. Osvenskii, O.G. Stolyarov, and L.P. Kholodnyi, Sov. Phys. Crystallogr. 18, 218 (1973).

4. D.E. Holmes, R.T. Chen, K.R. Elliott, and C.G. Kirkpatrick, Appl. Phys. Lett. 40, 46 (1982).

5. D.E. Holmes, R.T. Chen, K.R. Elliott, C.G. Kirkpatrick, and P.W. Yu, IEEE Trans. Electron Devices, ED-29, 1045 (1982).

6. L.B. Ta, H.M. Hobgood, A. Rohatgi, and R.N. Thomas, J. Appl. Phys. 53, 5771 (1982)

7. J.M. Parsey, Jr., Y. Nanishi, J. Lagowski, and H.C. Gatos, J. Electrochem. Soc. 128, 936 (1981); 129, 388 (1982).

8. J. Lagowski, H.C. Gatos, J.M. Parsey, K. Wada, M. Kaminska, and W. Walukiewicz, Appl. Phys. Lett. 40, 342 (1982).

9. M. Kaminska, M. Skowronski, M. Godlewski, and W. Kuszko, presented at 4th Lund Conference on Deep Level Impurities in Semiconductors, Eger, Hungary, May 1983.

10. E.R. Weber, H. Ennen, U. Kaufmann, J. Windscheif, J. Schneider, and T. Wosinski, J. Appl. Phys. 53, 6140 (1982).

11. M. Skowronski, M. Kaminska, and W. Kuszko, unpublished.

12. B.K. Meyer, D.M. Hoffmann, J.M. Spaeth, and F. Lohse, in this proceedings.

13. A.S. Jordan, R. Caruso, and A.R. Von Neida, The Bell System Technical Journal 59, 593 (1980).

14. M.G. Mil'vidskii, V.B. Osvensky, and S.S. Shifrin, J. Crystal Growth 52, 396 (1981).

15. G. Jacob, Semi-Insulating III-V Materials, edited by S. Makram-Ebeid and B. Tuck (Shiva, London, 1982) p. 2.

16. J. Lagowski, H.C. Gatos, T. Aoyama and D.Gl Lin, Appl. Phys. Lett., in press.

17. G.M. Martin, J.P. Farges, G. Jacob, and J.P. Hallais, J. Appl. Phys. 50, 2840 (1980).

18. E.J. Johnson, J.A. Kafalas, and R.W. Davies, J. Appl. Phys. 54, 204 (1983).

19. T. Figielski, submitted to Appl. Phys. A.

20. K.R. Elliott, Appl. Phys. Lett. 42, 274 (1983).

21. G.M. Martin, Appl. Phys. Lett. 39, 747 (1981).

22. M. Taniguchi and T. Ikoma, J. Appl. Phys. 54, 6448 (1983).

23. M. Taniguchi and T. Ikoma, Appl. Phys. Lett. 45, 69 (1984).

24. J. Lagowski, D.G. Lin, T. Aoyama, and H.C. Gatos, Appl. Phys. Lett. 44, 336 (1984).

25. D.E. Holmes and R.T. Chen, J. Appl. Phys. 55, 3588 (1984).

26. Y. Nanishi, S. Ishida and S. Miyazawa, Jpn. J. Appl. Phys. 22, L54 (1982).

27. D. Rumsby, R.M. Ware, B. Smith, M. Tyjberg, M.R. Brozel, and E.J. Foulkes, Technical Digest of 1983 GaAs IC Symposium, Phoeniz, Arizona (1983) p. 34.

28. M. Yokogawa, S. Nishine, M. Sasaki, K. Matsumoto, K. Fujita, and S. Akai, Jpn. J. Appl. Phys. 23, L339 (1984).

29. R.M. Logan and D.T.J. Hurle, J. Phys. Chem. Solids 32, 1739 (1971).

30. D.T.J. Hurle, J. Phys. Chem. Solids 40, 613 (1979).

31. G.M. Blom, J. Crystal Growth 36, 125 (1976).

32. J.M. Parsey, Jr., J. Lagowski, and H.C. Gatos, Proc. III-V Opto-Electronics Epitaxy and Device Related Processes, edited by V.C. Keramidas and S. Mahajan, The Electrochem. Soc., Inc. (Pennington, N.J, 1983) p. 61.

33. J.A. Van Vechten, J. Electrochem. Soc. 122, 423 (1975).

34. P.M. Petroff and L.C. Kimerling, Appl. Phys. Lett. 29, 461 (1976).

35. See for example, G. Schoek and W.A. Tiller, Phil. Mag. 5, 43 (1960).

36. G.B. Bachlet, M. Schlüter, and G.A. Baraff, Phys. Rev. B27, 2545 (1983).

37. P.J. Lin-Chung and T.L. Reinecke, Phys. Rev. B27, 1101 (1983).

38. P.W. Yu and D.C. Walters, Appl. Phys. Lett. 41, 863 (1982).

39. G. Vincent, D. Bois, and A. Chantre, J. Appl. Phys. 53, 3643 (1982).

40. We refer to EL2 as to a native deep donor which is a dominant midgap level in undoped or lightly doped Bridgman-grown GaAs, and which is the major defect level in MOCVD GaAs (41). Recently re-examined electron emission rate of this level is:

$$e^{-1} = \frac{3.53}{T^2} 10^{-8} \exp\left(\frac{9450}{T}\right) \text{sec}^{-1}$$

41. L. Samuelson, in this proceeding.

42. G. Jacob, M. Duseaux, J.P. Farges, M.M.B. Van der Boom, and P.J. Roksnoer, J. Crystal Growth 61, 417 (1983).

43. M. Duseaux and S. Martin, Proc. 3d Conf. on Semi-Insulating III-V Materials, Warm Springs, Oregon, April 1984, in press.

44. Y Seki, H. Watanabe, and J. Matsui, J. Appl. Phys. 49, 822 (1978).

45. P.A. Kirby, IEEE J. Quantum Electron. QE-11, 562 (1975).

46. V. Swaminathan and S.M. Copley, J. Appl. Phys. 47, 4405 (1967).

47. E.R. Weber; Proc. 3d Conf. on Semi-Insulating III-V Materials Warm Springs, Oregon, April 1984, in press.

EL2 AND RELATED DEFECTS IN GaAs--CHALLENGES AND PITFALLS

H. C. GATOS AND J. LAGOWSKI
Massachusetts Institute of Technology, Cambridge, MA 02139

ABSTRACT

The incorporation process of nonequilibrium vacancies in melt-grown GaAs is strongly complicated by deviations from stoichiometry, and the presence of two sublattices. Many of the microdefects originating in these vacancies and their interactions introduce energy levels (shallow and deep) within the energy gap. The direct identification of the chemical or structural signature of these defects and its direct correlation to their electronic behavior is not generally possible. We must, therefore, rely on indirect methods and phenomenological models and be confronted with the associated pitfalls. EL2, a microdefect introducing a deep donor level, has been in the limelight in recent years because it is believed to be responsible for the semi-insulating behavior of undoped GaAs. Although much progress has been made towards understanding its origin and nature, some relevant questions remain unanswered. We will attempt to assess the present status of understanding of EL2 in the light of the most recent results.

I. INTRODUCTION

The microdefect which introduces a midgap level, referred to as EL2, in melt-grown GaAs has a most profound potential importance in solid state electronics and optoelectronics, because it is generally considered responsible for the semi-insulating (SI) behavior of undoped GaAs [1,2]. Such material is an ideally suited basis for GaAs IC's. In the last five years no other aspect of semiconductor materials has received greater attention, on an international basis, than EL2 as it relates directly or indirectly to SI GaAs.

Actually, in the light of its high electron mobility the prospect of GaAs IC's fabricated on bulk SI GaAs has been the major contributor to the transformation of the strictly epitaxial GaAs device technology to a technology where bulk crystals became a fundamental factor. This transformation, however, must overcome immense complexities associated with the growth and characterization of GaAs crystals, i.e., a very high melting point (1238°C), two sublattices with numerous combinations of point defects, and a highly volatile constituent rendering readily possible significant deviations from stoichiometry which broaden the complexity of the point defect framework. Considering the fact that an average of five publications a year on the growth of GaAs from the melt was recorded through the 70's, (Chemical Abstracts) we must consider the progress made on bulk GaAs growth in the last five years as remarkable.

Similarly, considering the multitude and complexity of point defects and their interactions, very impressive progress has been made in the understanding of the nature and properties of some of the point defects, and particularly those of EL2, although a number of relevant questions remain unanswered [1,2]. Only two to three years ago the controversy on the nature and origin of EL2 and also on the pertinent properites or approaches and techniques best suited for its study was very acute. This type of situation generally reflects a stage of low level of knowledge which is usually characterized by unfounded strong convictions and followings. We believe that we are past that stage today. There is certainly no general agreement regarding all aspects of EL2. However, the various proponents and practitioners of particular approaches and techniques have begun to relate to each other's views and approaches. We believe that from such a mature stage of development, we can only go forward to rapid progress.

Mat Res Soc Symp Proc Vol 46 · 1985 Materials Research Society

II. GENERAL REMARKS

A key issue is often underemphasized, underestimated, overlooked or even unappreciated: The electronic characteristics of semiconductors (such as the carrier concentration, carrier mobility, excess carrier lifetime and carrier diffusion length) and particularly those of semiconductor compounds, can be striking modulated (by up to orders of magnitude) by relatively small variations in materials properties such as impurity contamination (intentional or inadvertent) deviations from stoichiometry, defect structure, and homogeneity. In turn, these materials properties are extremely sensitive to crystal growth parameters such as rates of growth, thermal gradients in the growth system, convective flow of the melt, and chemical reactions with the growth environment.

It is, thus, apparent that the results of the investigation of a specific electronic characteristic, e.g., EL2, in less than extensively characterized GaAs, could be entirely meaningless or at best nonrepresentative of the semiconductor GaAs. Actually, entirely different results are obtained from the seed-end to the tail-end of the same crystal.

It is now known that the concentration and distribution of EL2 depend on the method of growth, on the type and concentration of impurities, on the deviations from stoichiometry, on the thermal history of the crystal, and others (see Table 1). Still in question is the relationship of EL2 to dislocations, to strain and other factors. In commercial Czochralski (CZ) LEC GaAs other midgap levels besides EL2 have been reported [3]. In horizontal Bridgman (HB)-grown crystals usually only EL2 is found unless the crystals are heavily doped with oxygen [4]. In small diameter laboratory-grown CZ LEC crystal along with the main level EL2, occasionally, very small concentrations of other midgap levels are found. EL2 is the only midgap level in GaAs epitaxial layers grown by MOVPE [5].

The majority of the investigations on microdefects in GaAs have been carried out on commercial crystals for which little information on their thermal and other growth parameters is usually available. It is, thus, indeed very surprising that the existing controversy and confusion on a single electronic characteristic, such as EL2, is not of a much greater magnitude than it is, even if the measurements of all the various techniques were obtained under optimum experimental conditions.

In the present communication we will review the present status of some critical aspects of EL2 in the context of the most recent experimental and theoretical results. We will not attempt to elaborate on the details of experimental techniques and of specific results; we hope, however, to show the importance of interrelating the results of more than one experimental technique, the significance of the thermal history, and characterization of the material used, and the pitfalls, inherent in approaches and techniques that can readily contribute to misleading results.

III. THE ROLE OF THE CRYSTAL GROWTH PROCESS

It is now well established that the reproducible growth of high quality SI GaAs requires stringent control of the crystal growth parameters and especially of the melt stoichiometry and of the thermal gradients in the solidifying ingot. The major role of melt composition was demonstrated in 1981-82 when the research groups of Rockwell International [6,7] and Westinghouse R&D Laboratories [8] found that growth from melts slightly rich in arsenic yield SI GaAs crystals which have high electron mobilities, and are highly stable with respect to thermal annealing used in IC processing. These results had an immediate impact on GaAs IC technology. The beneficial effect of arsenic-rich growth conditions was clearly linked to an increase in the concentration of the native defect EL2. For the very first time in the semiconductor history a fundamental technological advantage was attained not by the elimination of native defects, but by the increase of their

Table 1. MIDGAP LEVELS IN GaAs GROWN BY DIFFERENT METHODS

Growth Method	Concentration cm^{-3}	Dominant Level	Additional Levels	Major Factor Upon Solidification	Major Factor Post-Solidification
HB	1 to 5 x 10^{16}	EL2 EL2	-- ELO(1)	arsenic pressure above the melt	slow cooling low thermal gradients
CZ LEC	0.3 to 2 x 10^{16}	EL2 EL2 and/or others(3)	ELO(2)	[As]/[Ga] in the melt	fast cooling, thermal gradients
VPE & MOVPE	0.1 to 5 x 10^{14}	EL2		[As]/[Ga] ratio in gas phase	low temperature
LPE	undetectable			Ga-rich conditions	low temperature
MBE	undetectable			very low growth temp.	very low temp

(1) heavily O-doped crystals
(2) small diameter crystals
(3) other midgap levels in large diameter crystals

concentration.

The understanding of the formation and nature of native defects in GaAs is intimately related to two stages of crystal growth [2]; (a) solidification phenomena, which take place at the solid-melt interface (or solid-gas interface in vapor phase growth); and (b) post-solidification phenomena which take place in the solidified material during subsequent cooling. The evolution of EL2 during GaAs growth involves both solidification and post-solidification phenomena. The various midgap levels (Table 1) in GaAs grown by different methods originate from differences in the characteristics of solidification and/or post-solidification processes.

Solidification-Related Phenomena

Solidification-related effects on native defects are determined by the following major factors: [2]

(a) elevated temperature necessary for crystal growth; it promotes atomic disorder which is metastably retained in the crystals.

(b) a finite existence region in which the Ga/As atom ratio in the solid can be different than one (deviation from stoichiometry).

(c) dynamic effects; i.e., pronounced variations in the microscopic growth rate which lead to the incorporation of defects at the growth interface.

The finite existence region is the dominant factor accounting for the increase of the EL2 concentration during growth from arsenic-rich melts. The results of the MIT group [9] (see Fig. 1) on horizontal Bridgman (HB) growth of GaAs with the melt stoichiometry varied by changing the temperature of the arsenic source, T_{As}, have shown that the concentration of EL2 increases with increasing partial As pressure over the melt (i.e., with increasing arsenic atom fraction in the melt). Similar EL2 behavior was also observed in LEC-grown GaAs [6-8]. In Fig. 2 we have summarized the literature data on EL2 as a function of [As]/[Ga] ratio in the gas phase for VPE- and MOVPE-grown GaAs layers [5,11-13]. Vapor phase growth takes place at about 700°C in contrast to melt growth at 1238°C. Thus, the epitaxial layers exhibit EL2 concentration 2 to 3 orders of magnitude lower than HB crystals. Nevertheless,

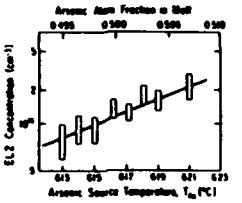

Fig. 1. EL2 concentration vs. melt composition for HB-grown GaAs.

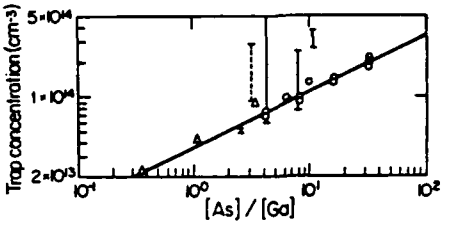

Fig. 2. EL2 concentration vs. [As]/[Ga] flux ratio during MOVPE growth. ○, △, I, & $\bar{I}$ after ref. 5,11,12, & 13, respectively.

an increase of EL2 concentration with increasing [As]/[Ga] ratio is evident in Fig. 2. Extrapolation of the VPE results of Fig. 2 to Ga-rich growth conditions representative of LPE growth (at a similar temperature range) leads to very low EL2 concentration consistent with experimental findings. Undetectable concentration of EL2 in MBE layers is a direct consequence of the very low growth temperatures at which the existence region vanishes.

Post-Solidification Processes

Post-solidification processes are related to two major factors [2]:

(a) supersaturation of the crystals with vacancies during cooling which migrate, recombine, interact, form complexes, coalesce into dislocations, and participate in dislocation climb.

(b) excessive thermal stresses in the cooling crystal which generate dislocations and point defects with an inhomogeneous distribution dictated by the stress fields.

For melt-grown GaAs the post-solidification defect interactions (factor a) can be identified and distinguished from processes taking place during solidification because they depend on the Fermi energy. At the melting point temperature, 1238°C, the Fermi level in GaAs is fixed at its intrinsic value and it cannot be changed by intentional doping at a level below $10^{18}cm^{-3}$. However, at lower temperatures experienced by the crystal during cooling, the intrinsic carrier concentration, n_i, decreases significantly, and moderate doping can be sufficient to vary the Fermi energy and thus change the charge state of the defects and their tendency to coalesce and migrate. The Fermi energy control of the EL2 concentration was demonstrated by the MIT group in 1981 [9,14]. In 1984 the same group [15] demonstrated the Fermi energy control of the coalescence of vacancy into dislocation loops. Both sets of results are summarized in Fig. 3 together with the corresponding Fermi energy change at a temperature of about 1100 K, which is believed to be a critical temperature in defect interactions.

It is seen in Fig. 3 that n-type doping at concentration exceeding $8x10^{16}cm^{-3}$ leads to a rapid decrease of the dislocation density and also to the suppression of the EL2 concentration. This effect, combined with the sensitivity of EL2 to the melt stoichiometry (Fig. 2) has led to the original assignment of EL2 to the arsenic antisite defect As_{Ga}. The MIT group [9,14] has proposed that the EL2 originates from the migration of the gallium vacancy V_{Ga} to a neighboring antisite, As_{As}, which creates the arsenic antisite (see Fig. 4):

$$V_{Ga}^{--} + As_{As} \rightleftarrows As_{Ga}^{+} + V_{As}^{+} + 4e^{-} \qquad (1)$$

Obviously, this reaction's path from left to right is rapidly suppressed by the increase of free electron concentration in accord with results of

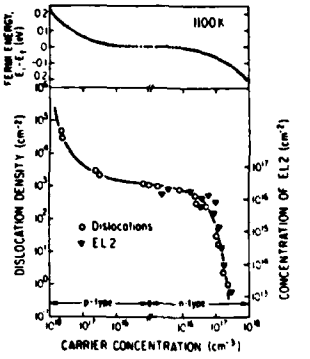

Fig. 3. See text.

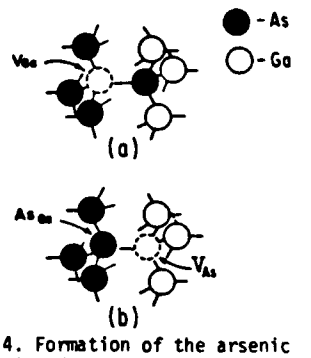

Fig. 4. Formation of the arsenic antisite due to migration of gallium vacancy.

Fig. 3. The monotonic increase of the EL2 concentration under As-rich melt growth (Fig. 1) is caused by the increased concentration of the gallium vacancies. As discussed in ref. 15, the Fermi energy-controlled migration of gallium vacancies (reaction 1) can also explain the dislocation density behavior shown in Fig. 3.

It should be noted that the association of EL2 with the As_{Ga} defect was simultaneously and independently proposed by the group of Shanghai Institute of Metallurgy [16] in conjunction with EL2 behavior in GaAs VPE and MOVPE layers.

It should be emphasized that the effects of the Fermi energy control of defects in epitaxial GaAs can be significantly different from that in the melt growth crystals. As discussed above, the high melting point temperature renders ineffective any Fermi energy control of the defect creation during the solidification process. Fermi energy control is effective in melt-grown GaAs only at lower temperatures (<1100 K). However, in VPE GaAs it can control the formation of defects as well as their subsequent migration, during the actual crystal formation. This difference between melt and VPE growth is significant as it permits the explanation of apparent contradictions between results of various research groups whereby the EL2 concentration is suppressed by n-type doping in melt-grown GaAs [9,17] and whereas it is enhanced by n-type doping (suppressed by p-type doping [5]) in VPE layers [17]. The defect interaction described by eqn. 1 can be taken as the same final step leading to the creation of EL2, in VPE growth as well. In VPE growth, however, n-type (p-type) doping will first of all increase (decrease) the equilibrium concentration of the acceptor-type gallium vacancies, since it is a general rule that the addition of donors (acceptors) will increase (decrease) the solubility of other acceptors (in this case gallium vacancies). If this effect is a dominant one, it will lead to dopant effects which are opposite to those observed in the melt-grown GaAs which are associated with the Fermi energy control of the migration of V_{Ga} (eqn. 1) rather than its initial concentration.

Effects of Thermal Stress

Excessive thermal stresses on the solidifying crystal can generate dislocations [18,19], antisite defects and other point defects and their complexes [20]. This additional channel of point defect generation is especially important during LEC growth of large diameter crystals. It leads to the generation of EL2 as well as other midgap levels of the EL2 family which are not observed in HB GaAs and in small diameter LEC GaAs crystals

grown by non-commercial groups. The spatial distribution of the stress-induced midgap levels follows the critical thermal stress pattern [21]. This pattern, however, does not necessarily represent the concentration distribution of just EL2. Thus, relationships between EL2 and the stress fields involve ambiguities discussed later in conjunction with the optical identification of EL2.

IV. IDENTIFICATION AND PROPERTIES

It is a common consensus that EL2 is related to the antisite defect As_{Ga}. This assignment has generated great interest in the study of antisite defects in GaAs and has brought to bear the use and correlation of different techniques in defect characterization. Thus, lines with symmetry consistent with that of As_{Ga} have been identified in GaAs by Electron Paramagnetic Resonance (EPR)[22], Electron Nuclear Double Resonance (ENDOR) [23] and high resolution optical measurements [24,25]. DLTS, [26] photocapacitance, [27,28], near infrared optical absorption [29,30], and photoluminescence [31] studies have determined energies, capture cross sections, and fundamental properties of the midgap levels. At the present, however, there is no general agreement on the EL2 and/or antisite properties determined by various methods or even by the same methods, in different laboratories [32-37]. Theory of deep level defects has been intensively applied to calculations of the electronic levels for As_{Ga}; however, the 0.3 eV spacing between the single and double donor levels of this defect seem to be the only undisputed result of the state-of-the-art calculations [38].

Transient Capacitance

It was believed up until recently that EL2 is the only midgap level present at appreciable concentrations in melt-grown GaAs. During the last two years it has been established with a high degree of confidence that other midgap levels are often present, especially in LEC GaAs (Table 1 and Fig. 5)

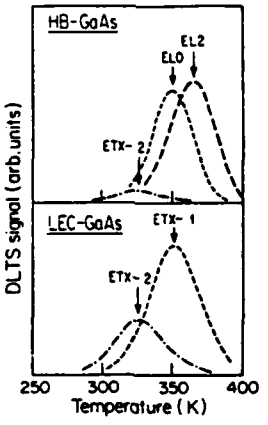

Fig. 5. DLTS spectra of midgap levels in GaAs grown by HB and LEC method. Emission rate window 25.6 s^{-1}. LEC results from ref. (3).

at concentrations which depend on the growth conditions [3,4, 39, 40]. Some of these levels exhibit very similar activation energies of the corrected thermal emission rates (T^2e^{-1}) but different values of capture cross sections. Such cases can lead to identification ambiguities by standard DLTS measurements and even by direct capacitance transient measurements. Commonly encountered interfering parameters (e.g., high ratios, N_T/N_D-N_A, of the deep level concentration, N_T, and the concentration of ionized impurities $N_D^+-N_A^-$ [41,43]; inhomogeneities in the semiconductor and/or rectifying contacts, excessive leakage current [44]; and effects of high electric field or recombination transients at low bias [45,46] can lead to artifacts such as non-exponential capacitance transients, shifts and broadening of the DLTS peaks which could either be mistaken as signals of additional deep levels or lead to erroneous deep level parameters.

In order to minimize the chances of DLTS misinterpretation, we propose to pursue the identification of slightly different midgap levels simultaneously present, by using short duration filling pulses. We have used

this technique successfully to distinguish between EL2 and the midgap level EL0 present in heavily oxygen-doped HB-GaAs [4,41,42]. (EL0 is not necessarily directly related to the oxygen impurity.) Both levels have almost identical energies, yet EL0 exhibits a capture cross section four times larger than that of EL2. As shown in Fig. 6a, in the "oxygen-free" crystals containing EL2 only, a decrease of the filling pulse duration leads only to a decrease in the peak height. In oxygen-doped GaAs shortening the duration of the filling pulse causes a shift of the DLTS peak to lower temperatures and a decrease of the peak half-width (Fig. 6b). This behavior is indicative of the presence of the two levels, EL2 and EL0. Due to its higher value of electron capture cross section, the relative contribution of EL0 to the overall DLTS signal is enhanced by short duration filling pulses, whereas that of EL2 is decreased.

Using the above types of DLTS measurements as well as direct analysis of capacitance transients, we have studied over 1000 samples from about 80 HB GaAs crystals and about 30 CZ-LEC crystals grown in our laboratory (all of a cross section of about 1 cm^2). We found that in all these crystals EL2 is the dominant level. Even in heavily oxygen-doped crystals the concentration of the second most important level, EL0, never exceeded that of EL2 [47]; in the majority of the crystals the EL0 concentration was about 10% of the EL2 concentration. We have utilized the results of our studies to revise the EL2 emission rate characteristics as shown in Fig. 7, where the revised emission rate plot of EL2 spans over 7 orders of magnitude. It is in excellent agreement with previous data obtained on MOVPE (ref 5) and bulk crystals.

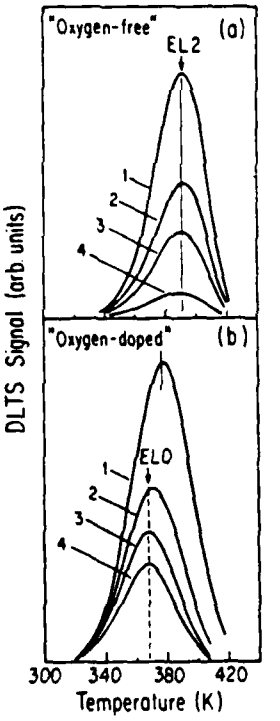

Fig. 6. DLTS spectra of midgap levels in (a) oxygen-free & in (b) heavily oxygen-doped Bridgman-grown GaAs. Spectra 1-4 correspond to decreasing filling pulse duration.

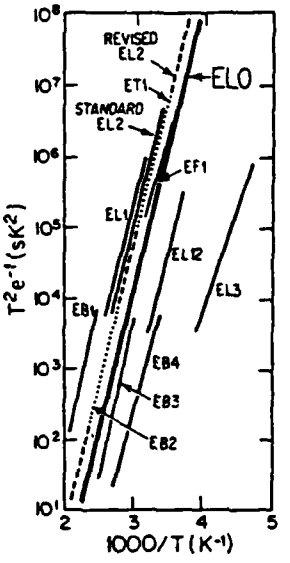

Fig. 7. Emission rate for deep electron traps in GaAs (see text).

The corresponding expression for the EL2 emission rate is: $e^{-1}(3.53\times10^{-8}/T^2)$ exp(9450/T) in sec^{-1}; this expression is slightly different than that assigned to EL2 and taken so far as the "standard"[26].

In view of a persisting controversy on the assignment of EL2 to As_{Ga} it is worth mentioning that transient capacitance measurements in GaAs have thus far failed to provide any evidence of the doubly charged deep state of EL2 [38]. Such a state must exist if EL2 is to be associated with As_{Ga}. It should be noted, however, that DLTS could not reveal the second EL2 level whether it is present or not. The proximity of the doubly charged state to the valence band (this state is expected to be about 0.3 eV below the standard EL2 level) makes its detection by Schottky barrier DLTS entirely impossible unless this state exhibits a highly unrealistic capture cross section ratio σ_n/σ_p exceeding 10^7.

In view of the above, extreme caution should be exercised in addressing this technique as powerful and unique. Used as commonly described and discussed, it can both generate nonexisting traps and fail to reveal existing trapping levels.

Optical Absorption

Optical absorption as shown in Fig. 8 is a characteristic feature of n-type and semi-insulating GaAs [29]. This structure is related to EL2. It was at first incorrectly assigned to photoionization transitions from EL2 to the conduction band minimum at the Γ, L and X points of the Brillouin zone (Fig. 8a) [28]. Correct interpretation of the spectrum includes the EL2 intracenter absorption band which extends from 1.03 to 1.3 eV and is responsible for the pronounced bulge at 1.2 eV in the overall absorption spectrum [30,43].

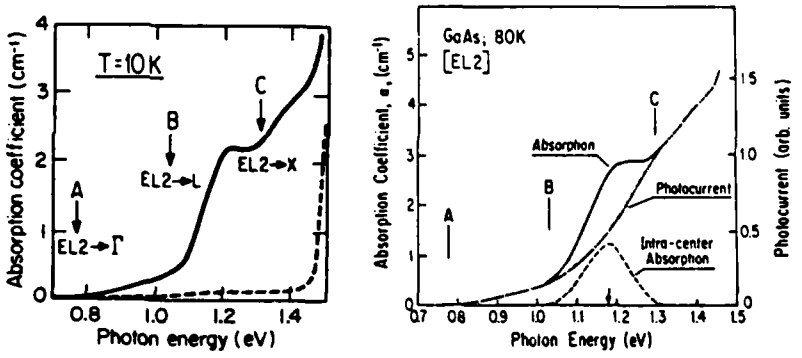

Fig. 8 (a) (b)
EL2-related optical absorption (see text).

The near infrared absorption coefficient calibrated as a function of the EL2 concentration (as determined from DLTS measurements) was used as a means for the optical determination of the EL2 concentration (ref. 29). A number of investigators have questioned the quantitative validity of the original calibration. Extensive optical studies in our laboratory on GaAs crystals containing also the midgap EL0 level have led to a revised calibration of the absorption coefficient. As discussed in an accompanying paper [43], N_T values were determined from transient capacitance measurements using an accurate procedure with correction factors derived for arbitrary values of $N_T/N_D^+-N_A^-$ and, thus suitable for the determination of large trap concentration. The use of standard correction factors (which are derived for $N_T \ll N_D^+-N_A^-$ leads to a significant underestimation of N_T values. Perhaps this could account for noticeable shift of the previous absorption calibration curve toward lower

concentrations of deep levels.*(See Fig. 9.)

Optical absorption is probably the most commonly used method for the determination of the EL2 concentration in semi-insulating GaAs on a macrocale, as well as on a microscale by absorption scanning [21,48] or by transmission imaging [49]. The method is convenient to use, and represents the only quantitative means for nondestructive determination of the EL2 concentration in SI GaAs. The distinct advantages of the technique and its widely accepted use notwithstanding, there are potential ambiguities that must not be overlooked, related not only to the use of an incorrect calibration factor, $d\alpha/dN_T$, but also to potential contribution of defects, other than EL2 to α. This latter factor is especially important in studies of the spatial distribution of EL2 in ingots and its correlation with other characteristics such as dislocations and thermal stress.

It is well known that excessive stress (thermal during postgrowth cooling, or intentionally applied to cause a plastic deformation) can change significantly the absorption spectrum of GaAs [50]. As shown in Fig. 10, the

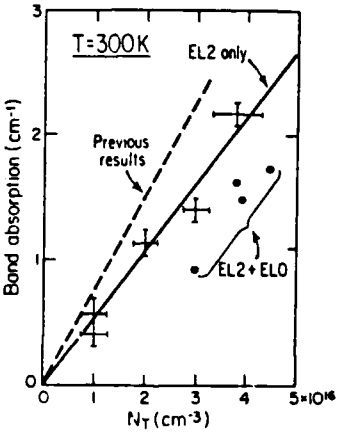

Fig. 9. Optical absorption at 300 K; λ = 1.06 μm vs. the concentration of midgap levels.

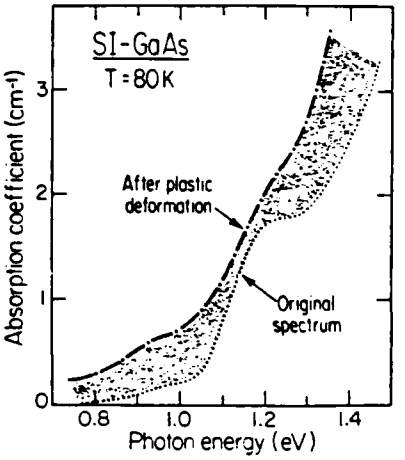

Fig. 10. Absorption changes induced in SI GaAs by plastic deformation.

the absorption in a deformed SI GaAs crystal is greater than in the predeformed crystal [51]. It is seen that the spectrum of the deformed crystal is not a quantitative displacement of the EL2 spectrum. It is, thus, apparent that the stress-induced increase of absorption is caused by the generation of defects other than EL2. It is also apparent that correspondence between absorption changes and stress distribution (or dislocation patterns) in LEC GaAs can be observed with precise measurements even if the EL2 distribution is uniform in the material. These interfering aspects are frequently overlooked, perhaps because of the belief prevailing in the past that EL2 is the midgap level solely responsible for many key properties of GaAs. In view of more recent results, this assumption need no longer be accepted. Careful re-examination of many results on optical measurements appears to be now necessary in order to separate apparent and real relationships between the EL2 and other characteristics.

*In an earlier study [47] employing simplified correction factors we have also underestimated the values of N_T which were much closer to those of ref. 29.

High resolution optical studies on EL2 intracenter transitions and on the corresponding no-phonon line have most recently provided a new insight into the relationship between EL2 and the neutral state of isolated As_{Ga} [43].

Optical Quenching (Bleaching) of EL2

Since 1977 EL2 has been known to exhibit optical quenching [52,27] which transfers the level into a metastable state resulting in quenching of the corresponding photocapacitance, and to the bleaching of the characteristic EL2 optical absorption, [28] as shown in Fig. 8a. This optical quenching has not as yet been adequately explained or understood; yet it has been taken as the "EL2" fingerprint, [29] i.e., a unique criterion for the identication of EL2. This interesting concept of "EL2 fingerprinting" was subsequently stretched far beyond its original ramifications. It became a common practice to treat quenching similar to that of EL2 as a unique evidence that the center involved is indeed EL2. At the same time, different quenching characteristics were considered as proof that the center involved is not EL2. A strong controversy has developed on this issue among various research groups. A large part of this controversy stems from pitfalls associated with the overstretched fingerprinting concept. We will illustrate relevant ambiguities with examples of considerable current interest involving quenching of the deep level photoluminescence, shallow level thermally stimulated current (TSC), and optically detected EPR lines of As_{Ga}.

Quenching of Photoluminescence

Deep level luminescence in SI GaAs and in p-type GaAs exhibits three rather broad bands (see Fig. 11) peaked at 0.64, 0.68, and about 0.8 eV; [53,54] all of them have been considered as potentially related to EL2. The photoluminescence study of ref. [55] has shown that under YAG laser illumination the low energy band exhibits a photo-induced persistent quenching effect. The spectral distribution of the quenching efficiency was found to be very similar to that of the photocapacitance quenching of the EL2 (see Fig. 12).

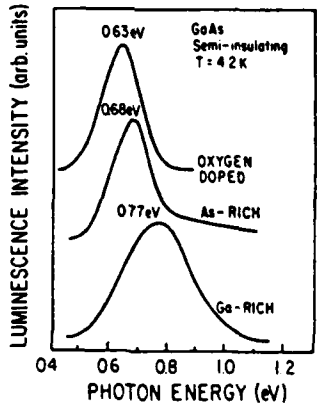

Fig. 11. Deep level luminescence bands in SI GaAs.

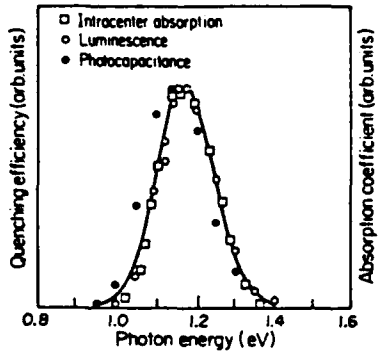

Fig. 12. See text.

This similarity was taken as evidence for the association of the low energy luminescence band with the EL2 level, despite the oxygen doping experiments,

implying quite different origin of the band [53,54]. The controversy was settled in a convincing manner by most recent experiments of time-resolved recombination at midgap levels [56]. This study has shown that the quenching of the 0.64 eV band is related to the EL2 quenching only indirectly, as it is due to the elimination of the excess carrier generation channel provided by EL2 absorption. The authors of ref. 56 have also pointed out that in principle, a decreased absorption related to optical bleaching of EL2 could result, under YAG excitation, in the decrease of the intensity of any deep photoluminescence band.

Quenching of Shallow Levels

Thermally stimulated current (TSC) measurements in SI GaAs [57] have recently led to the discovery of shallow levels which exhibited a metastable behavior under illumination with 1.18 eV photons (see Fig. 13) similar to that involved in the optical quenching of EL2. As in the case of EL2, recovery of the normal state of the optically quenched TSC peaks B_1, B_2 and C_5 was found to require heating to a temperature $T \geq 115$ K. The metastable behavior of the shallow levels was considered as evidence that these levels must be constituents of the various midgap levels in support of the charge-state-controlled structural relaxation model of EL2 [58].

As discussed elsewhere in these proceedings, [59] we have refuted these conclusions by comparing the integrated magnitudes of TSC peaks with the concentration of EL2. We have found that the upper concentration limit for shallow levels exhibiting metastable behavior was below $2\times10^{15}cm^{-3}$, which is significantly below typical concentrations of EL2 and EL0 in GaAs ($5\times10^{15}cm^{-3}$ to $4\times10^{16}cm^{-3}$). It thus appears appropriate to take the observed metastability of the shallow levels as evidence that IR quenching is not restricted to or uniquely related only to EL2, but in fact, it can be exhibited by other levels in GaAs.

Quenching of EPR and ODMR Lines of As_{Ga}

The studies pointed out above on luminescence and of TSC prove that photoquenching similar to that of EL2 should not be used as a decisive argument that a given defect is related to EL2. On the other hand, we can make the reverse argument: different photoquenching behavior than that of EL2 does not necessarily negate the relation between the defect and EL2.

In 1984 two groups reported on EPR and ODMR studies, which supported the association of EL2 with isolated As_{Ga} [34,36,60]. Two other groups, however, questioned this association [33,35,37,50]. They observed (a) that the concentration of As_{Ga} determined from EPR line intensity in plastically deformed GaAs is significantly larger than the concentration of EL2 determined from the absorption bleaching characteristics [50], and (b) that the EL2 absorption can be bleached completely while the ODENDOR signal of As_{Ga} remains practically unchanged [33,35,37] (see Fig. 14).

Arguments (a) and (b) could be used decisively against the association of EL2 with As_{Ga} if it were not for the fact that the two techniques, i.e., optical absorption on the one hand, and EPR or ODMR on the other, probe different charge states. As_{Ga} introduces two donor-type levels in gallium arsenide (see Fig. 15) corresponding to different charge states denoted as o/+ state and +/++ state. The EL2 optical absorption spectrum shown in Fig. 8 corresponds to electron transitions from the neutral As_{Ga}. Optical bleaching of the absorption and of the intracenter transitions measures the change in the concentration of neutral antisites. Furthermore, the photobleaching or photo-quenching process studied thus far would correspond to a metastable transition involving a neutral antisite only. It is very probable that photo-induced transfer into a metastable state is much less efficient for the ionized defect than for the neutral [61]. It is, however, this ionized antisite which contributes to the intensity of EPR and ODMR lines. Thus, if the neutral and the ionized antisites are simultaneously present

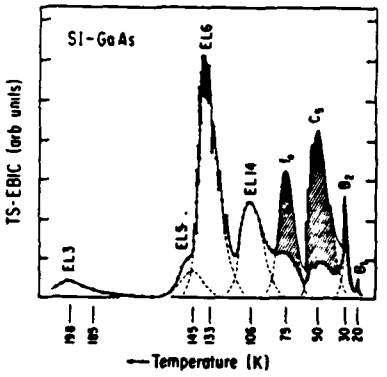

Fig. 13. TSC spectra of SI GaAs; (-) before quenching with 1.18 eV photons and (...) after quenching.

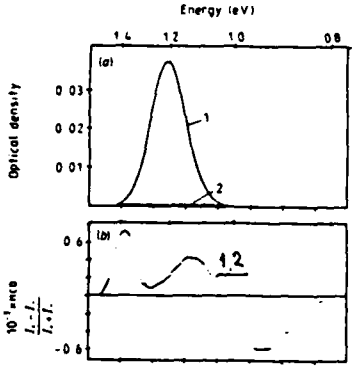

Fig. 14. (a) Intracenter EL2 absorption and (b) magnetic circular dichroism of As_{Ga}. 1 and 2 correspond to measurements made before and after irradiation with 1.18 eV photons.

in SI GaAs, the neutral ones will be effectively transferred into metastable states leading to absorption bleaching, while the majority of the charged antisites would remain in a normal paramagnetically active state.

The above potential explanation of the differences between EPR and optical absorption remains a hypothesis, unless differences between stable-metastable transitions are quantitatively determined for neutral and ionized EL2 states. Preliminary experiments on absorption and photoluminescence quenching in n- and p-type GaAs seem to indicate that quenching is indeed by far more efficient when EL2 is occupied [61].

EPILOGUE

The results and conclusions of the most recent studies, (with widely varying techniques), on deep levels in GaAs, and more specifically, on EL2 begin to converge in many important aspects. This is a clear sign of an improved understanding of the techniques employed, of the meaning of the experimental results and of an advanced theoretical framework of the phenomena involved. EL2 is according to most recent accounts related to As_{Ga}. It is no longer the only midgap level; there are certainly others, although of uncertain nature and/or origin. But EL2 remains the most important of midgap levels since it is primarily responsible for the semi-insulating behavior of GaAs.

There is, however, controversy still in the air regarding the assignment of EL2 to the isolated As_{Ga}. It is, of course, important to address, what we consider the basis of the remaining controversy. It is essentially based on studies and results involving the quenching and the associated metastable state of EL2 (and or other deep levels). Neither the quenching nor the metastability-related phenomena are as yet understood sufficiently well so that the evolution of a clear picture regarding the unambiguous meaning of quenching and metastability measurements is not as yet possible. As progress is made towards a better understanding of these phenomena not only the existing controversy will be settled, but the phenomena themselves will become effective factors in pursuing the study and understanding of point defects in GaAs and related materials.

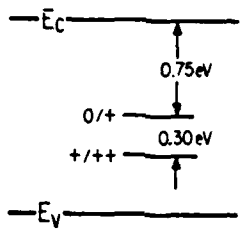

Fig. 15. Electronic levels of As_{Ga}. (Ref. 38)

ACKNOWLEDGMENT

The authors are grateful to the National Aeronautics and Space Administration, the Office of Naval Research, and the Air Force Office of Scientific Research for financial support.

REFERENCES

1. S. Makram-Ebeid, P. Langlade and G.M. Martin, in Semi-Insulating III-V Materials, Oregon, 1984, edited by D.C. Look and J.S.Blakemore, Shiva Publishing, Ltd., Nantwich, Cheshire CW5 5ES, England, 1984, p. 184.
2. J. Lagowski and H.C. Gatos, 13th Int. Conf. on Defects in Semiconductors, Coronado, CA, 1984, edited by L.C. Kimerling and J.M. Parsey, Jr., The Metallurgical Soc. of AIME, 1985, p. 73.
3. M. Taniguchi and T. Ikoma, J. Appl. Phys. 54, 6448 (1983).
4. J. Lagowski, D.G. Lin, T. Aoyama and H.C. Gatos, Appl. Phys. Lett. 44, 336 (1984).
5. L. Samuelson, P. Omling, H. Titze and H.G. Grimmeiss, J. Cryst. Growth 55, 164 (1981).
6. D.E. Holmes, R.T. Chen, K.R. Elliott and C.G. Kirkpatrick, Appl. Phys. Lett. 40, 46 (1982).
7. D.E. Holmes, R.T. Chen, K.R. Elliott and C.G. Kirkpatrick and P.W. Yu, IEEE Trans. Electron Devices, ED-29, 1045 (1982).
8. L.B. Ta, H.M. Hobgood, A. Rohatgi and R.N. Thomas, J. Appl. Phys. 53, 5771 (1982).
9. J. Lagowski, H.C. Gatos, J.M. Parsey, K. Wada, M. Kaminska and W. Walukiewicz, Appl. Phys. Lett. 40, 342 (1982).
10. W. Walukiewicz, J. Lagowski and H.C. Gatos, Appl. Phys. Lett. 43, 192 (1983).
11. M.D. Miller, G.H. Olsen and M. Ettenberg, Appl. Phys. Lett. 31, 538, (1977).
12. P.K. Bhattacharya, J.W. Ku, S.J.T. Owen, V. Aebi, C.B. Cooper and R.L. Moon, Appl. Phys. Lett. 36, 304 (1980).
13. Zhou Binglin, Wang Le, Shao Yongfu and Chen Qiyu, Acta Physica Sinica 28, 350 (1979).
14. M. Kaminska, J. Lagowski, J. Parsey, K. Wada and H.C. Gatos, GaAs and Related Compounds, 1981Inst. Phys. Conf. Ser. 63, 197 (1982).
15. J. Lagowski, H.C. Gatos, T. Aoyama and D.G. Lin, Appl. Phys. Lett. 45, 680 (1984).
16. Zou Yuanxi, GaAs and Related Compounds, 1981, Inst. Phys. Conf. Ser. 63, 185 (1982).
17. Zou Yuanxi, Zhou Jicheng, Mo Peigen, Lu Fengzhen, Li Liamsheng, Shao Jiuan, Huang Lei, Sun Henghui and Sheng Chi, Inst. Phys. Conf. Ser. 65, 49 (1983).

18. A.S. Jordan, R. Caruso and A.R. Von Neida, The Bell System Technical Journal 59, 593 (1980).
19. M.G. Mil'vidskii, V.B. Osvensky and S.S. Shifrin, J. Crystal Growth 52, 396 (1981).
20. E.R. Weber, H. Ennen, U. Kaufmann, J. Windscheif, J. Schneider and T. Wosinski, J. Appl. Phys. 53, 6140 (1982).
21. D.E. Holmes and R.T. Chen, J. Appl. Phys. 55, 3588 (1984).
22. R.J. Wagner, J.J. Krebs, G.M. Stauss and A.M. White, Solid State Commun. 36, 15 (1980).
23. D.M. Hofmann, B.K. Meyer, F. Lohse and J.M. Spaeth, Phys. Rev. Lett. 53, 1187 (1984).
24. M. Skowronski, M. Kaminska, W. Kuszko and M. Godlewski (1983) 4th Conf. on Deep Impurity Centers in Semiconductors, Eger, Hungary.
25. M. Kaminska, M. Skowronski, W. Kuszko, J. Lagowski, J. Parsey and H.C. Gatos, Czech. J. Phys. B34, 409 (1984).
26. For early compilation of DTLS results see: G.M. Martin, A. Mitonneau, and A. Mircea, Electron Lett. 13, 191 (1977).
27. G. Vincent, D. Bois and A. Chantre, J. Appl. Phys. 53, 3643 (1982).
28. A. Chantre, G. Vincent and D. Bois, Phys. Rev. B23, 5335 (1981).
29. G.M. Martin, Appl. Phys. Lett. 39, 747 (1981).
30. M. Kaminska, M. Skowronski, J. Lagowski, J.M. Parsey and H.C. Gatos, Appl. Phys. Lett. 43, 302 (1983).
31. See for example, M. Tajima, Jpn. J. Appl. Phys. 24, L47 (1985) and references therein.
32. See for example a discussion on EPR and ENDOR data in ref. 33-37.
33. B.K. Meyer, J.M. Spaeth and M. Scheffler, Phys. Rev. Lett. 52, 851 (1984).
34. M. Deiri, K.P. Homewood and B.C. Cavenett, J. Phys. C, Solid State Phys. 17, L627 (1984).
35. B.K. Meyer and J.M. Spaeth, J. Phys. C, Solid State Phys. 18, L99 (1985).
36. U. Kaufmann, Phys. Rev. Lett. 54, 1332 (1985).
37. B.K. Meyer, J.M. Spaeth and M. Scheffler, Phys. Rev. Lett. 54, 1333 (1985).
38. See G.A. Baraff, in Semi-Insulating III-V Materials, edited by D.C. Look and J.S. Blakemore, Shiva Publishing, Ltd., Nantwich, England, 1984, p. 416, and references therein.
39. M. Taniguchi and T. Ikoma, Appl. Phys. Lett. 45, 69 (1984).
40. P.W. Yue and D.C. Walters, Appl. Phys. Lett. 41, 863 (1982).
41. D. Stevenard, M. Lannoo and J.C. Bourgoin, submitted to Solid State Electronics, also see J.C. Bourgoin and D. Stevenard, Appl. Phys. Lett. 46, 311 (1985).
42. J. Lagowski, D.G. Lin, T. Aoyama and H.C. Gatos, Appl. Phys. Lett. 46, 312 (1985).
43. M. Skowronski, D.G. Lin, J. Lagowski, L.M. Pawlowicz, K.Y. Ko and H.C. Gatos, in this proceedings.
44. J. Lagowski, D.G. Lin, H.C. Gatos, J.M. Parsey, Jr., and M. Kaminska, Appl. Phys. Lett. 45, 89 (1984).
45. A. Mircea and A. Mitonneau, J. de Phys. Lett. F40, L31 (1979).
46. S. Makram-Ebeid and M. Lannoo, Phys. Rev. B25, 6406 (1982).
47. H.C. Gatos, M. Skowronski and J. Lagowski, Proc. of Inst. Conf. on GaAs and Related Compounds, Biarritz, France 1984, in press.
48. M.R. Brozel, I. Grant, R.M. Ware and D.J. Stirland, Appl. Phys. Lett. 42, 610 (1983).
49. P. Dobrilla, J.S. Blakemore and R.Y. Koyama, Semi-Insulating III-V Materials, edited by D.C. Look and J.S. Blakemore, Shiva Publishing, Ltd., edited by D.C. Look and J.S. Blakemore, Shiva Publishing, Ltd, Nantwich, England, 1984, p. 282.
50. L. Samuelson, P. Omling, E.R. Weber and H.G. Grimmeis, Semi-Insulating III-V Compounds, edited by D.C. Look and J.S. Blakemore, Shiva Publishing Ltd., Nantwich, England, 1984, p. 268.
51. F. Dabkowski, A. Hennel, J. Lagowski and H.C. Gatos, unpublished.
52. D. Bois and G. Vincent, J. Phys. Lett. 38, 351 (1977).

53. P.W. Yu, Solid State Commun. 43, 953 (1982).
54. P.W. Yu, Appl. Phys. Lett. 44, 330 (1984).
55. P. Leyral and G. Guillot, Semi-Insulating III-V Materials, edited by D.C. Look and J.S. Blakemore, Shiva Publishing, Ltd., Nantwich, England, 1982, p. 1tt.
56. D. Paget and P.B. Klein, 13th Int. Conf. on Defects in Semiconductors, Coronado, CA, 1984, edited by L.C. Kimerling and J.M. Parsey, Jr., Metall. Soc. of AIME, p. 959.
57. J. Fillard, J. Bonnafe and M. Castagne, Solid St. Commun. 52, 885 (1984).
58. M. Levinson, Phys. Rev. B28, 3660 (1983).
59. C.-J. Li, Q. Sun, J. Lagowski and H.C. Gatos, in this proceedings.
60. U. Kaufmann, J. Windscheif, M. Baemler, J. Schneider and F. Köhl, Semi-Insulating III-V Materials, edited by J.C. Look and J.S. Blakemore, Shiva Publishing, Ltd., Nantwich, England, 1984, p. 246.
61. M. Skowronski, J. Lagowski and H.C. Gatos, unpublished.

EBIC SPECTROSCOPY - A NEW APPROACH TO MICROSCALE CHARACTERIZATION OF DEEP LEVELS IN SEMI-INSULATING GaAs

C.-J. LI,* Q. SUN, J. LAGOWSKI AND H.C. GATOS
Massachusetts Institute of Technology, Cambridge, MA 02139

ABSTRACT

We propose a new approach to the defect characterization in semi-insulating (SI) GaAs which combines the high spatial resolution and scanning capability of the Electron Beam-Induced Current (EBIC) mode of Scanning Electron Microscopy (SEM) with the advantages of optical and thermal spectroscopies employed in the identification of deep levels. In the PHOTO-EBIC approach a DC electron beam and a chopped subbandgap monochromatic light impinge on the SI GaAs through a semi-transparent Au electrode. The photo-induced modulation of the EBIC as a function of the subbandgap energy of incident photons constitutes a structure which corresponds to the photoionization of deep levels. In the thermally stimulated EBIC (TS-EBIC) the deep levels are filled at low temperature by the excess carriers generated by an electron beam. Subsequently, the changes of EBIC as a function of temperature constitute a spectrum of peaks which correspond to different deep levels. The peak position determines the deep level energy while the magnitude of peaks can be used for the assessment of the relative concentration of deep levels located within the small volume probed by the electron beam.

INTRODUCTION

Microscale characterization of electronic defects in (SI) GaAs has been a challenging issue pertinent to materials problems encountered in GaAs IC technology. The low concentration of free carriers is the main obstacle which limits the applicability of high resolution electron beam methods such as EBIC and cathodoluminescence, CL. Up to now the distribution of electronic defects in SI material has been studied primarily by optical methods involving near infrared absorption measurements [1-3] (deep levels) or photoluminescence measurements [4] (shallow levels). The spatial resolution of these methods is poor, typically between 0.1 mm and 1 mm. Optical methods, however, constitute a means for the identification of electronic defects from the spectral characteristics of photoionization and radiative recombination processes.

In this paper we present a new photo-EBIC characterization approach which combines the spectroscopic advantages of optical methods with the high spatial resolution and scanning capability of EBIC. We discuss the experimental arrangement for photo-EBIC spectroscopy and for the deep and shallow level identification from thermally-stimulated EBIC spectra.

EXPERIMENTAL

The scanning electron microscope modified for electronic characterization studies is shown schematically in Fig. 1. It can operate in the standard SEM mode, in the EBIC modes (including photo-EBIC and TS-EBIC) and in the cathodoluminescence spectroscopy and scanning modes. The apparatus consists of: (a) an electron gun and electron beam focussing, scanning and blanking systems; (b) an optical illumination and collection system; and (c) a variable temperature cold stage, designed to operate at temperatures between 4.2 K and 300 K.

*Permanent address: Institute of Semiconductors, Chinese Academy of Sciences, Beijing, Peoples Republic of China.

Mat Res Soc Symp Proc Vol 46 1985 Materials Research Society

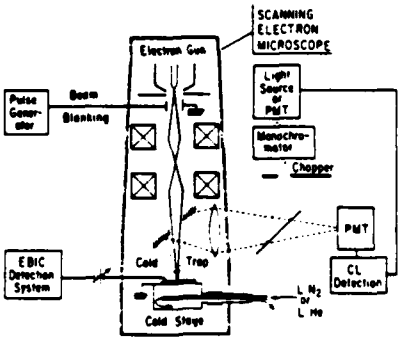

Fig. 1. Schematic representation of SEM apparatus adapted for CL, photo-EBIC, and TS-EBIC spectroscopies.

An additional cold trap was incorporated in the vicinity of the sample in order to reduce the carbon contamination of the surface.

An optical microscope incorporated into the SEM provided a means for the collection of the light emitted by the sample irradiated with the electron beam (cathodoluminescence). It was also used for the illumination of the sample with monochromatic light in the photo-EBIC measurements.

Commercial SI GaAs grown by the LEC method was employed in this study. A thin semi-transparent Au electrode was evaporated on the front surface of the samples (exposed to an electron beam and/or to incident light). A probing beam (DC) generated an EBIC signal between the Au electrode and the electric contact to the sample. In photo-EBIC spectroscopy the current changes induced by a chopped monochromatic light were recorded (using a lock-in amplifier) as a function of the energy of incident photons. High resolution EBIC and cathodoluminescence microprofiling were achieved by scanning an electron beam within a small sample region (<500 μm). Profiling over larger distances was realized by moving the sample stage while keeping the electron beam stationary. Spatially resolved TS-EBIC measurements were carried out by irradiating small selected areas of the sample with a stationary electron beam focussed to a 1 μm to 5 μm diameter spot.

RESULTS AND DISCUSSION

Cathodoluminescence

An initial assessment of the presently employed SI GaAs was performed using standard cathodoluminescence measurements. Readily detectable cathodoluminescence (CL) signals were obtained only at the liquid helium temperature. High resolution cathodoluminescence imaging revealed a typical cellular structure consisting of bright and dark regions commonly observed in SI GaAs [5]. The CL spectrum consists of two lines, i.e., the near bandgap line, B, at $h\nu \approx 1.515$ eV and the carbon line, C, at $h\nu \approx 1.495$ eV [5,6]. The ratios of the CL peak intensity, C/B, were very similar within the bright and the dark regions. It is, thus, very likely that the cellular structure of CL distribution in SI GaAs is not necessarily related to nonuniform carbon distribution, as recently suggested [5]. This structure probably originates in the nonuniform distribution of non-radiative recombination centers. Typical cathodoluminescence line scans of the carbon peak, C, and of the bandgap peak, B, are shown in Fig. 2a and 2b, respectively. They exhibit striking similarities consistent with the dominant role of spatial variations in the nonradiative recombination.

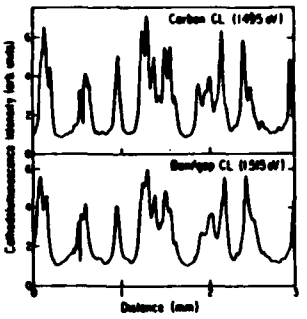

Fig. 2. CL scans of the carbon line, 1.495 eV, and near-bandgap line, 1.515 eV in undoped SI GaAs grown by the LEC method. Measurements were carried out at 4.2 K.

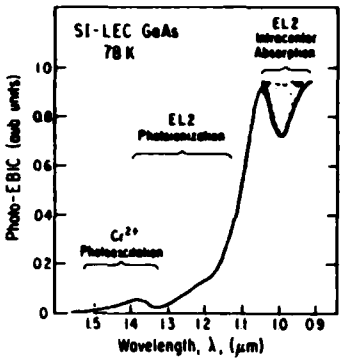

Fig. 3. Photo-EBIC spectrum of undoped SI GaAs which reveals midgap level transitions and the contribution from residual Cr impurity.

Photo-EBIC

For SI GaAs the EBIC is undetectably small in the dark. Under illumination the EBIC current becomes readily measurable. In Fig. 3 a typical sub-bandgap photo-EBIC spectrum of SI GaAs is shown, taken at 78 K using a 30 kV electron beam 5 μm in diameter and a beam 5 μm in diameter and a beam current of about 10^{-7} A.

We suggest the following interpretation of this spectrum:

1. The dominant photo-EBIC increase in the spectral range 1.3 to 1.1 μm is associated with EL2 photoionization [1,7].

2. The photo-EBIC minimum between 1.1 μm and 0.93 μm (shaded area in Fig. 3) is due to *EL2 intracenter* transitions which in themselves do not lead to the generation of free carriers [7].

3. The small peak at about 1.37 μm is probably associated with a photo-excitation of residual Cr^{2+} [8]. The presence of residual Cr impurity in undoped LEC GaAs may be surprising. However, on several occasions we have found Cr present (using independent measurements of optical absorption and DLTS) in commercial GaAs crystals claimed to be "undoped".

The magnitude of the photo-EBIC signal and its spatial variations are controlled primarily by two factors: (1) the net photoionization rate of deep levels under optical excitation; and (2) the recombination rate of excess carriers generated by the electron beam. The spatial resolution (lateral) of photo-EBIC microprofiling with respect to factor (1) is determined by the size of the light spot (about 40 μm in our experiments). The resolution with respect to factor (2) can be much better, typically between 1 μm and 10 μm, depending on the electron beam spot size or on the minority carrier diffusion length (whichever is larger).

Linear scans of photo-EBIC measured at 78 K for $\lambda = 1.06$ μm and $\lambda = 1.37$ μm, are shown in Fig. 4a and 4b, respectively. Scan "c" is the cathodoluminescence intensity measured at 78 K along the same scanning line.

Very pronounced inhomogeneities are seen in all scans. It is also seen that the photo-EBIC variations are very similar for both wavelengths of the incident light. Furthermore, the photo-EBIC profiles are quite similar to the cathodoluminescence profile. These similarities imply that spatial variations are very similar for both wavelengths of the incident light.

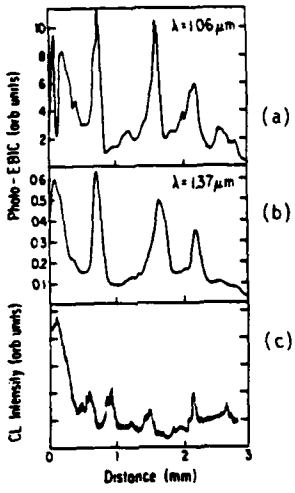

Fig. 4. Photo-EBIC scans and corresponding cathodoluminescence scans of SI GaAs. Measurements carried out at 78 K.

Furthermore, the photo-EBIC profiles are quite similar to the cathodoluminescence profile. These similarities imply that spatial variations of photo-EBIC and cathodoluminescence are of the same origin, i.e., they are caused predominantly by spatial variations in the concentration of recombination centers.

Thermally Stimulated EBIC

Deep level identificaton in SI GaAs is often carried out using thermally stimulated current (TSC) spectroscopy [9,10]. This technique can be effectively extended to microscale measurements by employing electron beam excitation rather than standard optical excitation.

At low temperatures (liquid nitrogen or liquid helium temperatures) the electron beam is focussed on a 1 μm - 5 μm diameter spot of the SI sample. The beam generates excess carriers which are confined within an effective excitation volume defined by the beam energy and the diffusion length of the excess carriers. Electron (hole) traps (deep levels) located within this volume become filled by the excess electrons (holes). The sample is subsequently heated, and the EBIC is monitored as a function of temperature and time. In SI GaAs this thermally stimulated EBIC corresponds to the thermal release of carriers from traps.

Typical EBIC as a function of temperature spectra are shown in Fig. 5. They exhibit a series of peaks which correspond to different deep levels. As in the standard TSC spectroscopy, the peak temperature can be used for the determination of the trap energy position, while the peak magnitude (or more precisely the current integrated over the time) provides a relative measure of the trap concentration. The two TS-EBIC spectra shown in Fig. 5, solid and dotted lines, correspond to electron beam irradiated spots separated by 100 μm. All other experimental conditions were kept the same. Thus, the differences between the spectra reflect differences in trap concentrations at two neighboring locations. The most significant concentration changes (by as much as a factor of 2) are observed for the shallow traps B_2, C_5, and f_0. Large variations in concentration of trap EL6 are also observed, however, in an opposite phase than those of the shallow traps; this trap is the second most important trap in bulk Gaas, and its concentration is often comparable to EL2 concentration. It should be pointed out that all of the traps seen in Fig. 5 have been previously identified in GaAs (see refs. 9 and 10).

Levels EL6 and C_5 exhibited low frequency oscillations of thermally stimulated current when dc electric fields applied to the sample exceeded 500 V/cm. In Fig. 5 these oscillations appear as a fine structure superimposed on the EL6 and C_5 peaks. The presence of TSC oscillations is significant. It differentiates EL6 and C_5 from other traps and implies that they exhibit a configurational energy barrier or a repulsive potential barrier[12].

The levels B_1, B_2, and C_5 have recently been shown to exhibit a metastable behavior (under illumination with 1.18 eV photons), similar to that involved

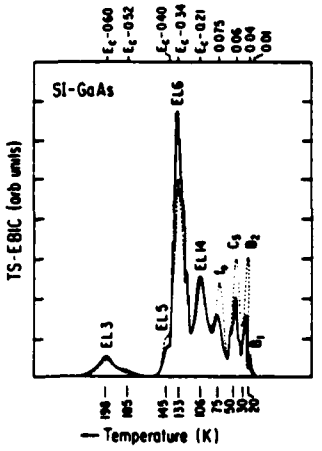

Fig. 5. Thermally stimulated EBIC spectra of SI GaAs. Solid and dotted line spectra were obtained from two spots of the sample separated by 100 μm. Fine oscillations superimposed on C_5 and EL6 peaks are real (see text).

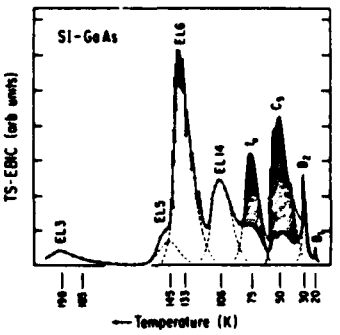

Fig. 6. Infrared quenching of TS-EBIC in SI GaAs. The original (solid line) spectrum was obtained with electron beam irradiation only. The quenched (dotted line) spectrum was obtained after additional IR illumination (see text).

in the optical excitation of EL2 into a metastable state [11]. As in the case of EL2, the recovery of the normal state of the B_1, B_2 and C_5 levels was found to require heating to a temperature ≥ 115 K.

The metastable behavior of the shallow traps leads to the IR quenching of the TSC peaks, which can be readily seen in the TS-EBIC spectra of Fig. 6. The solid line spectrum with pronounced B_2, C_5, and f_0 peaks was obtained using 5 min irradiation with 30 kV electron beam at 4.2 K. After irradiation the sample was kept for 2 min in the dark prior to increasing the temperature. The quenched spectrum (dotted line) was obtained when the 5 min electron beam irradiation was followed by 2 min illumination with an infrared light of $h\nu < 1.15$ eV (white light passing through a Si filter). All other conditions were exactly the same. The quenched peaks B_2, C_5, and f_0 could not recover their original magnitude upon subsequent bandgap illumination or electron beam irradiation. Their magnitude, however, could easily be restored by heating of the sample.

The metastable behavior of the shallow levels has been considered in ref. 11 as evidence that these levels are "constituents" of the various midgap levels of the "EL2 family." It has also been implied that the metastable and the stable configurations of EL2 correspond to the metastable and stable configurations of the shallow traps consistent with the model for the EL2 structural relaxation which is controlled by the charge state of the component shallow and deep defects [13].

In order to verify these conclusions we have estimated an upper concentration limit for the shallow traps by using the integrated magnitudes of the respected peaks relative to the magnitude of the EL6 and the upper limit of the EL6 concentration, $\leq 10^{16}$ cm^{-3} found in GaAs. We have obtained the following concentration upper limits: 10^{14}cm^{-3}, 5×10^{14}cm^{-3}, 2×10^{15}cm^{-3} and 1×10^{15}cm^{-3} for B_1, B_2, C_5 and f_0, respectively. The estimated concentrations are noticeably below typical concentrations of EL2 and EL0 in GaAs (5×10^{15}cm^{-3} to 4×10^{16}cm^{-3}). It is thus very unlikely that the shallow traps are constituents of the midgap level centers.

Accordingly, it appears appropriate to take the observed metastability of the shallow levels as clear evidence that IR quenching is not restricted to or uniquely related only to EL2, but in fact, it is exhibited by many other levels in GaAs, both deep [14] and shallow.

In summary, we have presented a new approach to the study of the distribution of energy levels in SI GaAs by employing photo- and EBIC spectroscopy. Photo-EBIC is a convenient means for semi-quantitative microscale studies. TS-EBIC, although time-consuming, constitutes a unique method for the determination of quantitative microscale profiles of the energy levels and their concentrations in GaAs.

ACKNOWLEDGEMENT

The authors are grateful to the Air Force Office of Scientific Research and to the National Aeronautics and Space Adminstration for financial support.

REFERENCES

1. G.M. Martin, Appl. Phys. Lett. 39, 747 (1981).
2. D.E. Holmes, R.T. Chen, K.R. Elliott, and C.G. Kirkpatrick, Appl. Phys. Lett. 43, 305 (1983).
3. M.R. Brozel, I. Grant, R.M. Ware and D.J. Stirland, Appl. Phys. Lett. 42, 610 (1983).
4. M. Yokogawa, S. Nishine, M. Sasaki, M. Matsumoto, K. Fujita and S. Akai, Jpn. J. Appl. Phys. 23, L339 (1984).
5. B. Wakefield, P.A. Leigh, M.H. Lyons and C.R. Elliott, Appl. Phys. Lett. 45, 67 (1984).
6. M. Tajima, Jpn. J. Appl. Phys. 21, L227 (1982).
7. M. Kaminska, M. Skowronski, J. Lagowski, J.M. Parsey and H.C. Gatos, Appl. Phys. Lett. 43, 302 (1983).
8. A.M. Hennel, S. Szuszkiewicz, M. Balkanski, G. Martinez and B. Clerjaud, Phys. Rev. B 23, 3933 (1981).
9. M.G. Buehler, Solid St. Electronics 15, 69 (1972).
10. G.M. Martin, in Semi-Insulating III-V Materials, edited by G.J. Rees, Shiva Publishing Ltd., Orpington, UK, 1980, p. 13.
11. J.P. Fillard, J. Bonnafe and M. Castagne, Solid St. Communications 25, 855 (1984).
12. M. Kaminska, J.M. Parsey, J. Lagowski and H.C. Gatos, Appl. Phys. Lett. 41, 989 (1982).
13. M. Levinson, Phys. Rev. B. 28, 3660 (1983).
14. M. Taniguchi and T. Ikoma, Appl. Phys. Lett. 45, 69 (1984).

Identification of a vanadium-related level in liquid encapsulated Czochralski grown GaAs

C. D. Brandt, A. M. Hennel, L. M. Pawlowicz, F. P. Dabkowski, J. Lagowski, and H. C. Gatos
Massachusetts Institute of Technology, Cambridge, Massachusetts 02139

(Received 5 May 1985; accepted for publication 21 June 1985)

We present the first positive identification of a vanadium-related electron trap in V-doped GaAs crystals grown by the liquid encapsulated Czochralski technique in pyrolytic boron nitride crucibles. Detailed deep level transient spectroscopy and capacitance transient analysis yielded a trap energy of 0.15 ± 0.01 eV below the conduction band and an electron capture cross section of about 2×10^{-14} cm^2. Optical absorption and mobility data show that this level corresponds to the ionized acceptor state $V^{2+}(3d^3)$ of substitutional vanadium. No midgap levels other than EL2 could be detected in these V-doped crystals showing that doping with vanadium plays no direct role in the compensation process in semi-insulating GaAs crystals.

The growth of semi-insulating (SI) GaAs crystals has long been known to be intimately related to the controlled introduction of compensating deep levels near the middle of the energy gap. Doping with chromium to create a deep acceptor level or control of the melt stoichiometry to create the deep native defect donor EL2 have become standard growth techniques. Due to its high diffusivity, chromium tends to accumulate at the GaAs surface during heat treatment, producing thin conducting layers detrimental to device fabrication. Efforts to improve the thermal stability of SI GaAs have produced several studies on V-doped GaAs which indicated that vanadium has a lower diffusivity than chromium.[1-3]

Electron paramagnetic resonance (EPR) and optical absorption studies[4] of transition metal impurities in III-V compounds have shown that the most probable location of elemental vanadium is on a gallium site. A single acceptor level $V^{3+}(3d^2)/V^{2+}(3d^3)$ can be predicted to be in the upper third of the energy gap,[5] while the position of the vanadium donor level $V^{4+}(3d^1)/V^{3+}(3d^2)$ is uncertain. Studies utilizing deep level transient spectroscopy (DLTS) techniques[6,7] have thus far failed to positively identify a vanadium-related level in bulk GaAs. Optical absorption[8] and EPR studies[1,8] indicated the presence of the neutral V^{3+} charge state; however, these studies were unable to identify the energy position of a vanadium-related level in bulk crystals. A vanadium-related hole trap at $E_v + 0.58$ eV was suggested for vapor phase epitaxially grown GaAs[9] although this trap has not been observed in melt grown crystals. An early Hall-effect analysis[10] indicated a vanadium-related level in liquid encapsulated Czochralski (LEC) GaAs at about 0.2 eV below the conduction band.

In the present study we identified a vanadium-related electron trap in melt-grown GaAs by both DLTS and capacitance transient analysis. The samples studied were cut from LEC GaAs crystals grown in this laboratory using pyrolytic boron nitride crucibles from melts doped with high purity elemental vanadium to a level of 3×10^{19} cm^{-3}. In addition, selenium doping of the melt up to about 9×10^{16} cm^{-3} was used to ensure n-type conducting material. The samples exhibited the following carrier concentration n and mobility μ values: $n = 2\text{–}6 \times 10^{16}$ cm^{-3}, $\mu = 2800\text{–}3100$ cm^2/Vs at 77 K and $n = 3\text{–}8 \times 10^{16}$ cm^{-3}, $\mu = 3400\text{–}3700$ cm^2/Vs at 300 K. Ohmic contacts were fabricated using an In-Sn alloy, and evaporated gold was used for the Schottky barrier.

The features of our transient capacitance system pertinent to this study include (a) precise temperature control and monitoring in the range 15–420 K, (b) direct emission rate measurements over a range 10^{-3}–10^4 s^{-1} from capacitance relaxation recorded with a signal averager, and (c) standard DLTS mode operation using a boxcar averager.

Typical DLTS spectra in the range 100–420 K for crystals with and without vanadium are shown in Fig. 1. The dominant midgap level EL2 is clearly visible in both spectra at ~390 K having a concentration of about 2×10^{16} cm^{-3}.

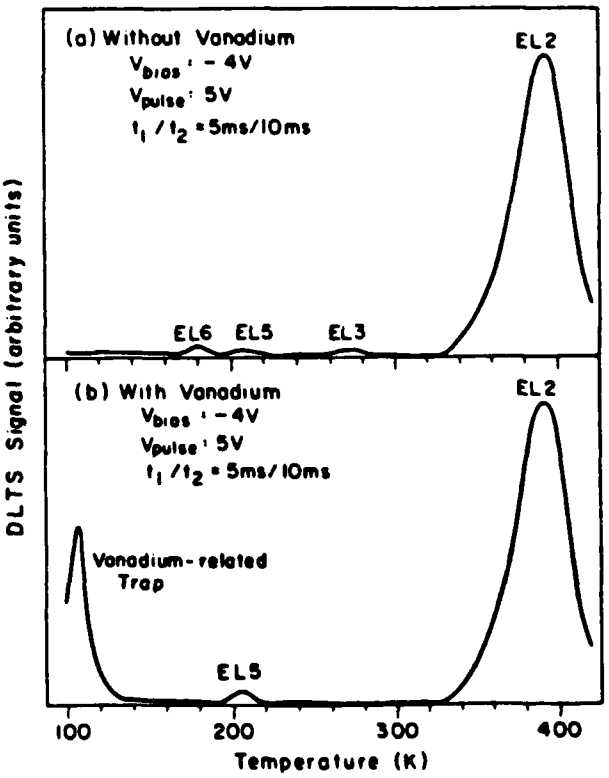

FIG. 1. DLTS spectra of n-type LEC-grown GaAs (a) without and (b) with vanadium doping. Bias − 4 V, filling pulse amplitude 5 V, t_1/t_2 = 5 ms/10 ms.

 0003-6951/85/180607-03$01.00

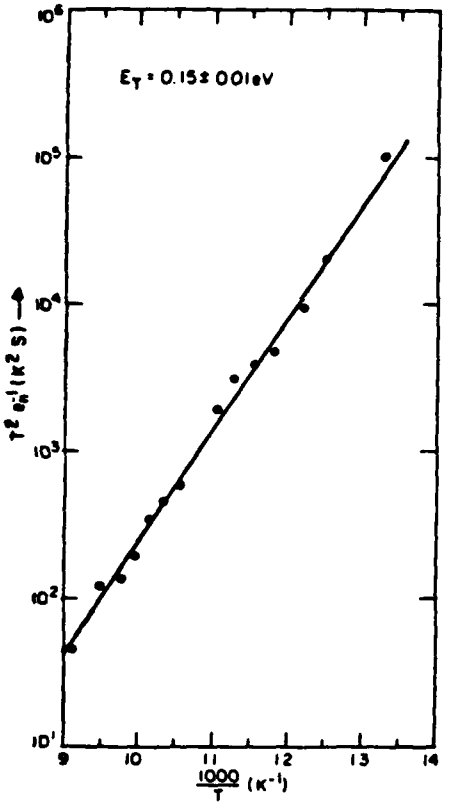

FIG. 2. Emission rate thermal activation plot $T^2 e_n^{-1}$ vs $10^3/T$ for vanadium-related electron trap in LEC-grown GaAs.

No additional midgap levels could be detected. In the V-doped material however, a new well-pronounced peak appeared at ~100 K, indicating the presence of a new electron trap. This temperature is close to the low-temperature limit of standard nitrogen expansion cryostats; accordingly a more precise analysis of this level was carried out using a Joule–Thompson closed-cycle helium cryostat. Capacitance transients caused by electron emission from this trap were measured as a function of temperature, enabling the calculation of the activation energy, electron capture cross section, and the concentration of this level. In Fig. 2 we present the thermal activation plot of the emission rate (e_n) as a function of temperature for this vanadium-related level. Previous studies[11] have shown that this type of emission rate versus temperature plot can be used as a convenient signature of deep levels. A least-squares analysis yielded an activation energy of 0.15 ± 0.01 eV and an electron capture cross section of about 2×10^{-14} cm^2. Though a defect level of similar energy was recently reported in some melt-grown crystals,[12] DLTS spectra of over 100 nonvanadium-doped horizontal Bridgman and LEC GaAs crystals grown in this laboratory do not reveal any deep levels of this activation energy and capture cross section. A compilation of previous DLTS studies[11] did not reveal a 0.15-eV electron trap in melt-grown GaAs. A 0.15-eV level was mentioned as being vanadium related in a subsequent review[13]; however, no justification for this assignment was given.

An important aspect of this vanadium-doped material is that the 77 K mobility is lower than that at 300 K. Hall measurements on GaAs crystals grown under identical conditions but without the addition of vanadium yielded mobilities of 5000 cm^2/Vs at 300 K and 9800 cm^2/Vs at 77 K, i.e., noticeably higher than those of V-doped crystals. Doping with vanadium also resulted in a decrease in the free-electron concentration. These results indicate that vanadium is acting as an acceptor in accord with theoretical predictions for the V^{2+} level.[5] Optical absorption studies on these V-doped crystals[14] show the characteristic absorption spectrum (see Fig. 3) recently identified as due to substitutional vanadium.[7,8] This spectrum originates from the intracenter transition $^3A_2(^3F) \rightarrow {}^3T_1(^3F)$ involving the unoccupied vanadium acceptor $V^{3+}(3d^2)/V^{2+}(3d^3)$. The intensity of this spectrum correlates well with the level of vanadium doping in these crystals. However, we have found that this absorption spectrum vanishes with increasing occupation of the $E_c - 0.15$ eV level brought about by intentional raising of the Fermi energy through additional selenium doping. This finding supports the identification of the 0.15-eV trap as being due to the acceptor state of substitutional vanadium.

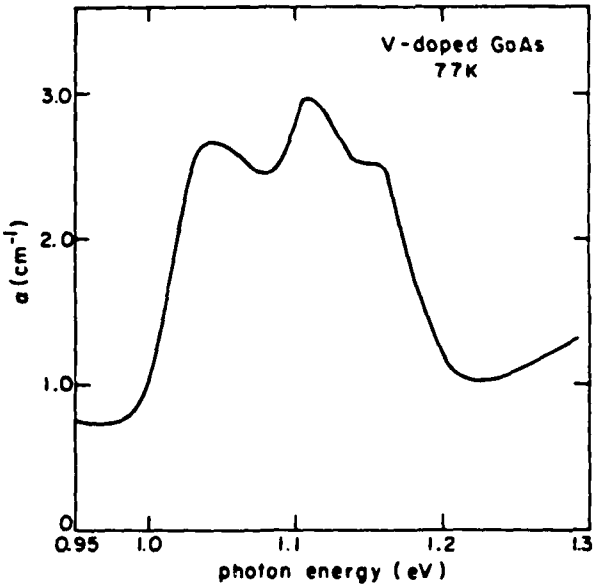

FIG. 3. Optical absorption spectrum of V-doped GaAs showing the $^3A_2(^3F) \rightarrow {}^3T_1(^3F)$ intracenter transition of the unoccupied vanadium acceptor $V^{3+}(3d^2)/V^{2+}(3d^3)$.

By examining individual capacitance transients of separate samples cut from the same boule, the concentration of this vanadium acceptor level was found to vary from 7.8×10^{15} cm^{-3} at the seed to 1.1×10^{16} cm^{-3} towards the tail in good agreement with the 10^{16} cm^{-3} obtained from the optical absorption intensity of vanadium. These values enable us to estimate the effective distribution coefficient of elemental vanadium in melt-grown GaAs to be about $k_{\text{eff}} = 2 \times 10^{-4}$. This value agrees with previously reported values of 7×10^{-4} and 5×10^{-4}.[1,3]

In summary, we have identified an electron trap in melt-grown GaAs directly related to elemental vanadium. This trap, located at 0.15 eV below the conduction band, corresponds to the V^{3+}/V^{2+} single acceptor level. The proximity of this level to the conduction band and the absence of any vanadium-related midgap levels indicate that the vanadium doping of LEC GaAs grown in pyrolytic boron nitride crucibles cannot lead to SI material. Further studies to ascertain

the potential involvement of vanadium, perhaps in the form of complexes with other impurities, in producing SI GaAs are in progress.

The authors are grateful to the Air Force Office of Scientific Research and the I.B.M. Corporation for financial support.

[1]U. Kaufmann, H. Ennen, J. Schneider, R. Worner, J. Weber, and F. Kohl, Phys. Rev. B 25, 5598 (1982).
[2]A. V. Vasilev, G. K. Ippolitova, E. M. Omelyanovskii, and A. I. Ryskin, Sov. Phys. Semicond. 10, 341 (1976).
[3]W. Kutt, D. Bimberg, M. Maier, H. Krautle, F. Kohl, and E. Bauser, Appl. Phys. Lett. 44, 1078 (1984).
[4]U. Kaufmann and J. Schneider, Adv. Electron. Electron Phys. 58, 81 (1983).
[5]M. J. Caldas, A. Fazzio, and A. Zunger, Appl. Phys. Lett. 45, 671 (1984).
[6]F. Litty, P. Leyral, S. Loualiche, A. Nouailhat, G. Guillot, and M. Lannoo, Physica B 117/118, 182 (1983).
[7]A. Mircea-Roussel, G. M. Martin, and J. E. Lowther, Solid State Commun. 36, 171 (1980).
[8]B. Clerjaud, C. Naud, C. Benjeddou, G. Guillot, P. Leyral, B. Deveaud, and B. Lambert, in *Semi-Insulating III-V Materials*, edited by D. C. Look and J. S. Blakemore (Shiva, Kah-nee-ta, 1984), p. 484.
[9]H. Terao, H. Sunakawa, K. Ohata, and H. Watanabe, in *Semi-Insulating III-V Materials*, edited by S. Makram-Ebeid and B. Tuck (Shiva, Nantwich, 1982), p. 54.
[10]R. W. Haisty and G. R. Cronin, in *Proceedings of the 7th International Conference on the Physics of Semiconductors*, edited by M. Hulin (Dunod, Paris, 1964), p. 1161.
[11]G. M. Martin, A. Mitonneau, and A. Mircea, Electron. Lett. 13, 191 (1977).
[12]D. C. Look, D. C. Walters, and J. R. Meyer, Solid State Commun. 42, 745 (1982).
[13]U. Kaufmann and J. Schneider, in *Landolt–Bornstein Numerical Data and Functional Relationships in Science and Technology*, edited by O. Madelung (Springer, Berlin, 1982), Vol. 17a, p. 231.
[14]A. M. Hennel, C. D. Brandt, H. Hsiaw, L. M. Pawlowicz, F. P. Dobkowski, J. Lagowski, and H. C. Gatos (unpublished).

Native hole trap in bulk GaAs and its association with the double-charge state of the arsenic antisite defect

J. Lagowski, D. G. Lin, T.-P. Chen, M. Skowronski, and H. C. Gatos
Massachusetts Institute of Technology, Cambridge, Massachusetts 02139

(Received 10 July 1985; accepted for publication 13 August 1985)

We have identified a dominant hole trap in *p*-type bulk GaAs employing deep level transient and photocapacitance spectroscopies. The trap is present at a concentration up to about 4×10^{16} cm^{-3}, and it has two charge states with energies 0.54 ± 0.02 and 0.77 ± 0.02 eV above the top of the valence band (at 77 K). From the upper level the trap can be photoexcited to a persistent metastable state just as the dominant midgap level, EL2. Impurity analysis and the photoionization characteristics rule out association of the trap with impurities Fe, Cu, or Mn. Taking into consideration theoretical results, it appears most likely that the two charge states of the trap are the single and double donor levels of the arsenic antisite As_{Ga} defect.

Deep levels associated with native defects in bulk GaAs crystals grown from the melt have been the subject of extensive studies,[1-3] motivated on one hand by the key of deep levels in the compensation of semi-insulating material used for integrated circuits,[2] and on the other hand, by the need for increasing the fundamental understanding of defect properties in III-V compounds.[3] Experimental studies of defects in bulk GaAs have been thus far carried out primarily on *n*-type and semi-insulating crystals. The deep levels located in the lower half of the energy gap and acting as hole traps in *p*-type GaAs have not been studied in any systematic manner except in epitaxial layers and regarding certain heavy metal impurities (Cu, Fe, Cr).[1]

In this letter we identify a dominant hole trap in *p*-type GaAs crystals grown from the melt, and we report the properties of this trap such as energy levels, emission rate, and photoionization spectra. Our findings bear directly on currently most actively pursued problems of native defects in GaAs, namely, on the electronic properties of the arsenic antisite, As_{Ga}, defect,[3-6] and on the nature of the major midgap donor EL2.

The present study was carried out on a series of GaAs crystals grown by the horizontal Bridgman method under conditions ensuring optimum melt stoichiometry[7] and negligible thermal stress. The crystals were doped with Zn to obtain free-hole concentration of about $(5–10)\times10^{16}$ cm^{-3}; the hole mobility was $\mu_p \simeq 200–300$ cm^2/Vs at 300 K. The concentration of residual impurities which can introduce hole traps (primarily Fe, Cr, Cu, Mn, Mg) and thus can interfere with the study of native hole traps, was determined using secondary ion mass spectroscopy (SIMS).[8] The upper concentration limits of these impurities were found to be about 3×10^{15}, 1×10^{15}, 5×10^{14}, 8×10^{14}, and 1×10^{15} cm^{-3}, respectively. These concentrations are about one order of magnitude smaller than the typical concentration of the hole trap ($2–4\times10^{16}$ cm^{-3}) discussed below. The corresponding *n*-type crystals were grown under exactly the same conditions, but without Zn doping, contained one midgap level EL2, located about 0.75 eV below the bottom of the conduction band. Other midgap levels (often referred to as the "EL2 family"),[9] if present, had concentrations not exceeding 3×10^{15} cm^{-3}.

The transient capacitance (and photocapacitance) measurements were carried out on Al-Schottky diodes evaporated on the *p*-type GaAs samples. We found it much more difficult to prepare Schottky diodes with good characteristics (breakdown voltage exceeding 4 V and leakage current at 4 V reverse bias below 1 mA/cm^2) on bulk *p*-type GaAs than on *n*-type GaAs. Accordingly, diodes of low leakage current suitable for deep level transient spectroscopy (DLTS) measurements were selected, by trial and error, from a large number of diodes prepared on the $(\bar{1}\bar{1}\bar{1})$ surfaces (*B* surfaces) of each sample. The capacitance changes were measured with a 1-MHz capacitance bridge, and in addition to the standard DLTS measurements, they were monitored as a function of time using a signal averager. The samples were placed on the cold finger of a variable temperature cryostat with provision for backside diode illumination (photocapacitance spectroscopy).

A typical transient capacitance spectrum of *p*-type bulk GaAs is shown in Fig. 1. It reveals one dominant deep hole trap which we denote as HM1. The corresponding hole emission rate thermal activation plot for this trap is also given in Fig. 1. It yields an activation energy $E_A = 0.52\pm0.01$ eV and a hole capture cross section $\sigma_{p^-} = (1\pm0.5)\times10^{-15}$ cm^2. The emission rate values given in Fig. 1. were calculated from the half time of the capacitance decay, $\tau_{1/2}$, as $e^{-1} = \tau_{1/2}/\ln 2$.

Fe in GaAs introduces a deep acceptor corresponding to

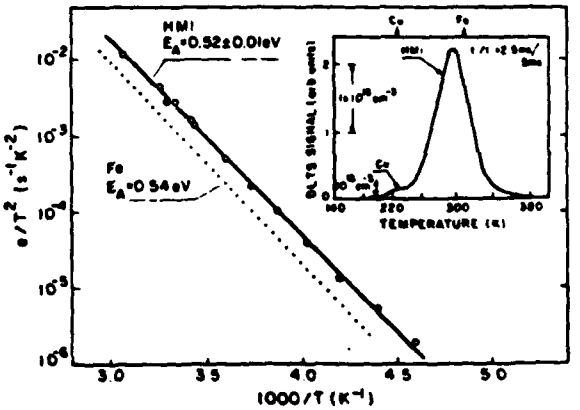

FIG. 1. DLTS spectrum (insert) and thermal activation plot of the hole emission rate of the HM1 trap. Emission rate for the Fe level is also shown after Ref. 10.

 0003-6951/85/210929-03$01.00

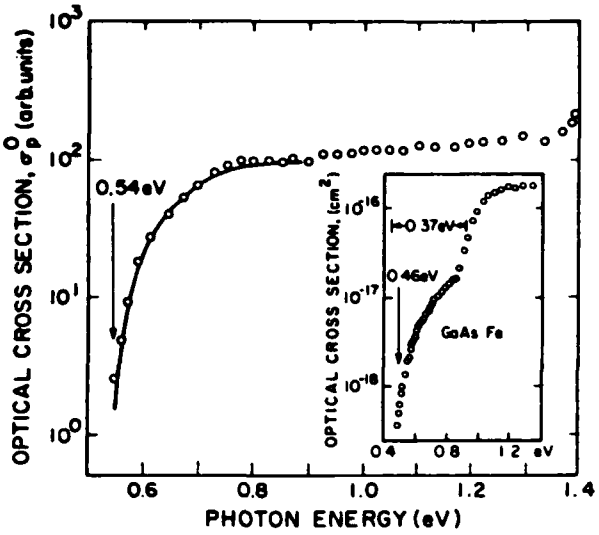

FIG. 2. Optical cross section for the first hole photoionization from HM1 trap to the valence band at 77 K; points—experimental, line—theoretical. (100 on the vertical scale corresponds to about 10^{-17} cm^2.) Insert shows photoionization cross section of Fe level (after Ref. 10).

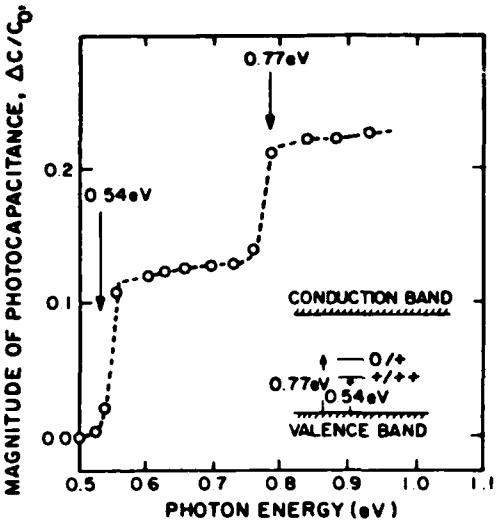

FIG. 3. Low-temperature (77 K) spectrum of steady-state photocapacitance.

Fe^{2+}/Fe^{3+} state with a thermal energy for emission of holes of about 0.54 eV,[10] i.e., very similar to the HM1 trap (Fig. 1). Such proximity makes the distinction between HM1 and Fe level difficult. In the present case SIMS analysis indicated an Fe upper concentration limit of $2-3\times10^{15}$ cm^{-3} in the investigated crystals, i.e., about one order of magnitude smaller than that of HM1. This low Fe concentration was confirmed by low-temperature photocapacitance spectroscopy measurements presented in Fig. 2. On the left-hand side of Fig. 2 the 80 K spectrum of the optical cross section, σ_p^0, for the photoexcitation of holes from the deep traps to the valence band is presented. The values of σ_p^0 were determined in a standard way from the initial slope of the capacitance transient $\Delta C/\Delta t\,|_{t\to0}$ (normalized to a constant photon flux) following the onset of illumination at temperatures sufficiently low to prevent thermal discharge of deep traps. The spectrum reveals only one low-energy threshold at $E_0\simeq0.54\pm0.02$ eV. This behavior is markedly different than that of σ_p^0 for Fe also shown in Fig. 2 (after Ref. 10). The 0.46- and 0.85-eV thresholds in the Fe spectrum correspond to the photoionization of holes from the ^5E ground state and $^5T_2$ excited state, respectively, of the same $3d^6$ configuration split by the crystal field. Using the optical cross-section values for the photoionization of the $^5T_2$ state ($\sigma_{Fe}^0\simeq2\times10^{-16}$ cm^2 at $h\nu\simeq1.2$ eV) we can estimate the upper concentration limit of Fe in our crystals assuming that the entire increase of the optical cross section ($\Delta\sigma_p^0\simeq3\times10^{-17}$ cm^2) between the 0.85 and 1.2 eV is brought about by the photoionization of the $^5T_2$ state. Such estimation yields $[Fe]<N_T\times\Delta\sigma_p^0/\sigma_{Fe}^0\simeq3\times10^{15}$ cm^{-3} ($N_T\simeq2\times10^{16}$ cm^{-3} is the concentration of the hole trap); this concentration is the same as that obtained by SIMS analysis. The σ_p^0 spectrum in Fig. 2 corresponds to transitions from the HM1 trap which was filled with holes by a saturating pulse of forward bias prior to illumination.

The threshold energy value $E_0=0.54\pm0.02$ eV was determined by fitting the low-energy tail of $\sigma_p^0(h\nu)$ to a standard energy dependence $\sigma_p^0\sim(h\nu-E_0)^{1.5}/(h\nu)^3$ for allowed transitions[11] (solid line in Fig. 2). This value is in good agreement with the emission rate activation energy of the HM1 trap. The presence of only one threshold over a wide energy region (up to 1.4 eV) indicates that HM1 is the only contributing trap. This trap, however, is a double-charge center capable of releasing one hole or two holes. The release of the second hole obviously cannot be observed in measurements of the initial photocapacitance slope because in the initial stages of photoionization only the first hole is released. The second ionization, however, is readily seen to take place at 0.77 eV in a spectral dependence of the magnitude of the steady-state photocapacitance on photon energy shown in Fig. 3. Here the diode with the traps filled was biased in the reverse direction ($C=C_0$) and illuminated with a monochromatic light. When the capacitance reached a steady-state value, C_s, the photon energy was increased, and the capacitance transient was recorded again. The relative magnitude of the capacitance change was defined as $\Delta C/C_0=[C_s(h\nu)-C_0]/C_0$.

The results of Figs. 2 and 3 clearly indicate the involvement of one center with two charge-state levels separated by an energy of about 0.23 ± 0.04 eV. As shown in the insert in Fig. 3, the low-energy threshold corresponds to the photoionization of a hole from the lower energy level to the valence band and the 0.77-eV threshold corresponds to the photoionization of the second hole from the trap. The above characteristics of the center are strikingly similar to those of the As_{Ga} defect. Theoretical calculation indeed predicts two charge-state levels for the As_{Ga}, separated by 0.25 eV.[12] The major midgap level EL2 in GaAs (commonly studied in n-type GaAs) has been identified with the single donor state of the arsenic antisite (0/+).[3] The lower double donor state (+/++) can be, with reasonable certainty, identified with the presently discovered HM1 trap. This assignment is consistent with a previous electron paramagnetic resonance (EPR) study of the arsenic antisite in plastically deformed GaAs.[6] However, the energy of +/++ state of about 0.47 eV (i.e., 0.05–0.07 eV below present value) was only roughly estimated from a weak photoenhancement of the

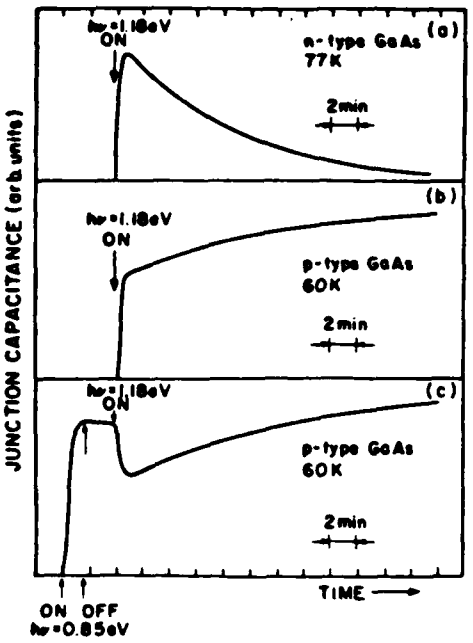

FIG. 4. Capacitance transient corresponding to deep level photoexcitation to the persistent metastable state for (a) *n*-type and (b) and (c) *p*-type GaAs.

EPR signal. The presence of a second charge state of EL2 at about 0.45 eV above the valence band was also proposed in a recent photocapacitance study of *n*-type liquid encapsulated crystal (LEC)-grown GaAs.[13]

Our identification of 0.54- and 0.77-eV levels with the two charge states of the As_{Ga} (EL2 being the higher energy state) is further supported by the persistent metastable behavior of the trap. In Fig. 4 curve (a) represents the well-known photocapacitance quenching effect in *n*-type GaAs with a characteristic overshot of the capacitance transient.[14] The initial fast increase of the capacitance is caused by photoionization of EL2, while the subsequent slow decrease corresponds to the EL2 transition to a metastable state; the metastable state is electrically neutral; accordingly, the final capacitance value coincides with the value prior to illumination. The photon energy of 1.18 eV leads to the maximum rate of transition to the metastable state.

In *p*-type GaAs the trap is originally positively charged and its transition to a neutral metastable state should lead to an increase in capacitance; this effect is opposite to that in *n*-type GaAs. The behavior is indeed seen in Fig. 4(b). After the transition is completed, the photosensitivity of the diode is diminished, especially with respect to the second photoionization process involving the $(0/+)$ state. Subsequently, 1.18 eV photons ionize the center leading to a rapid capacitance decrease followed by a slow transfer to the neutral metastable state. As in the case of *n*-type GaAs, the normal state can be recovered by increasing the temperature and/or by applying a long duration filling pulse.

In summary, the identification of a native hole trap in GaAs associated with a double charge donor provides the missing experimental link for establishing a working model of the As_{Ga} defect and understanding its role in the presence and in the characteristics of the dominant deep levels in GaAs.

The authors are grateful to the National Aeronautics and Space Administration and to the U.S. Air Force Office of Scientific Research for financial support.

[1]G. F. Neumark and K. Kosai, "Deep Levels in Wide Band-Gap III-V Semiconductors," in *Semiconductors and Semimetals*, edited by R. K. Willardson and A. C. Beer (Academic, New York, 1983), Vol. 19, p. 1.
[2]S. Makram-Ebeid, P. Langlade, and G. M. Martin, in *Semi-Insulating III-V Materials, Oregon, 1984*, edited by D. C. Look and J. S. Blakemore (Shiva, Cheshire, England, 1984), p. 184.
[3]J. Lagowski and H. C. Gatos, in *Defects in Semiconductors, Coronado, CA, 1984*, edited by L. C. Kimerling and J. M. Parsey, Jr. (The Metallurgical Society of AIME, Warrendale, PA, 1985), p. 73.
[4]B. K. Meyer and J. M. Spaeth, J. Phys. C **18**, L99 (1985).
[5]U. Kaufman, Phys. Rev. Lett. **54**, 1332 (1985).
[6]E. R. Weber, H. Enness, U. Kaufman, J. Windscheif, Y. Schneider, and T. Wosinski, J. Appl. Phys. **53**, 6140 (1982).
[7]J. M. Parsey, Y. Nanishi, J. Lagowski, and H. C. Gatos, J. Electrochem. Soc. **129**, 389 (1982).
[8]SIMS analysis was carried out by Charles Evans and Associates, San Mateo, California.
[9]M. Taniguchi and T. Ikoma, J. Appl. Phys. **54**, 6448 (1983).
[10]M. Kleverman, P. Omling, L.-A. Ledebo, and M. G. Brimmeiss, J. Appl. Phys. **54**, 814 (1983).
[11]G. Lucovsky, Solid State Commun. **3**, 299 (1965).
[12]G. A. Baraff, in *Semi-Insulating III-V Materials, Oregon, 1984*, edited by D. C. Look and J. S. Blakemore (Shiva, Cheshire, England, 1984), p. 416 and references therein.
[13]T. Wosinski, Appl. Phys. A **36**, 213 (1985).
[14]G. Vincent, D. Bois, and A. Chantre, J. Appl. Phys. **53**, 3643 (1982).

END

11-86

DTIC